A general model for energy hub economic dispatch

Published source:
Soheil Derafshi Beigvand, Hamdi Abdi, Massimo La Scala, A general model for energy hub economic dispatch, Applied Energy, Volume 190, 2017, Pages 1090-1111,ISSN 0306-2619, https://doi.org/10.1016/j.apenergy.2016.12.126.

A General Model for Energy Hub Economic Dispatch

Soheil Derafshi Beigvand[a], Hamdi Abdi[a,*], Massimo La Scala[b]

[a]*Electrical Engineering Department, Engineering Faculty, Razi University, 67149-67346 Kermanshah, Iran*
[b]*Electrical and Electronic Department (DEE), Polytechnic School of Bari (Politecnico di Bari), Bari, Italy*

Abstract–This paper proposes a new optimization algorithm, namely Self-Adoptive Learning with Time Varying Acceleration Coefficient-Gravitational Search Algorithm (SAL-TVAC-GSA), to solve highly nonlinear, non-convex, non-smooth, non-differential, and high-dimension single- and multi-objective Energy Hub Economic Dispatch (EHED) problems. The presented algorithm is based on GSA considering three fundamental modifications to improve the quality solution and performance of original GSA. Moreover, a new optimization framework for economic dispatch is adapted to a system of energy hubs considering different hub structures, various energy carriers (electricity, gas, heat, cool, and compressed air), valve-point loading effect and prohibited zones of electric-only units, as well as the different equality and inequality constraints. To show the effectiveness of the suggested method, a high-complex energy hub system consisting of 39 hubs with 29 structures and 76 energy (electricity, gas, and heat) production units is proposed. Two individual objectives including energy cost and hub losses are minimized separately as two single-objective EHED problems. These objectives are simultaneously minimized in the multi-objective optimization. Results obtained by SAL-TVAC-GSA in terms of quality solution and computational performance are compared with Enhanced GSA (EGSA), GSA, Particle Swarm Optimization (PSO), and Genetic Algorithm (GA) to demonstrate the ability of the proposed algorithm in finding an operating point with lower objective function.

Keywords–Economic dispatch, energy hub, energy hub economic dispatch, gravitational search algorithm, self-adoptive learning with time varying acceleration coefficient-gravitational search algorithm, optimization.

1. Introduction

Future vision of energy networks including several energy carriers in the form of multi-carrier systems [1] (also, called multiple energy carrier networks [2] or hybrid systems [3]), allows more flexibility in the integrated network operation and optimization [4,5]. In fact, various infrastructures can affect each other in terms of energy flow, storage, etc. In the meantime, energy hubs play an essential role in the connection points between different infrastructures allowing energy flow through various networks. Combination of several converters in hubs provides necessary motivations to integrate multiple energy carriers [3]. Some converters such as CHP devices [6–9] and tri-generations [10–13] in the hubs are two attractive cases which can establish more effective energy conversion between different carriers [1,3,4,6].

[*] Corresponding author. Hamdiabdi, hamdiabdi@rai.ac.ir, Tel.: +98 833 4283261; fax: +98 833 4283261.

In this regards, other elements (such as heater exchangers) may operate with a single carrier. In this view point, various carriers can be consumed by different hub structures to provide different forms of energy at the output port.

Proposing the different optimization problems for electrical systems will be lead to introduce two problems, namely Multi-Carrier System Optimal Power Flow (MCSOPF) and Energy Hub Optimal Dispatch (EHOD), for hybrid systems. The first one, optimizes the energy flow through various networks based on a desirability e.g. energy cost, emission cost, energy loss, and etc. [1,2,4]. So, the system condition in terms of all control and state variables, energy flows and the other quantities can be determined. Due to different structures associated with various energy infrastructures, the MCSOPF is a non-convex, non-smooth, nonlinear, and high-dimension optimization problem. Therefore, finding the global optimum could not to be guaranteed [3]. The EHOD optimizes a single hub neglecting the energy transmission losses [2]. The basic questions which should be answered by EHOD are how much of the available carriers at the input port of a hub should be consumed and how should they be converted in order to satisfy the demands at the hub outputs. In other words, this optimization process determines the optimal energy input subject to energy flow through the hub and load supplying.

The work presented in [2], introduces the hub concept and its modeling and optimizes a hybrid system including electrical and gas networks. The MCSOPF problem in [2] provides a general formulation which can be employed for various electrical and pipeline systems. In this context, [1] applied a decomposition method to MCSOPF. This approach uses virtual units and dummy variables to construct the problem. This makes a complex OPF problem involved with additional variables and constraints. An energy flow optimization of hybrid systems based on a modified version of teaching-learning algorithm has been reported in [4]. This reference optimizes multicarrier system including electrical, gas, and heat infrastructures. Authors of [3], analyzed the impact of heating systems on hybrid networks in terms of OPF. Another method based on employing an appropriate set of dependent variables has been proposed in [14]. In fact, in order to convert irregular equations into a regular set, it eliminates the addition of any new variable. A similar approach has been reported in [15]. In [16], a Gravitational Search Algorithm with Time Varying Acceleration Coefficient (TVAC-GSA) has been applied to MCSOPF problem. This method is based on the gravitational law and law of motion. In [17], multi-agent systems are used to optimize and control multiple energy carriers. The work reported in [18], studies the interactions in district electricity and heating systems. A combined analysis of these grids can be found in [19]. Optimal operation of integrated electrical and heating systems to accommodate the intermittent renewable sources has been proposed in [20]. Ref. [21] presented a model for integrated analysis of electricity, heat and gas networks. A similar work to form an integrated OPF for multiple energy networks has been developed in [22].

Ref. [2] suggested EHOD problem of an energy hub and described the related optimization process. Effect of energy hubs on the hybrid systems has been discussed in [23]. A generic framework for modeling of energy systems based on the hub concept has been suggested in [24]. In [25], a medium-term energy hub management based on electricity price as well as wind uncertainty has been documented. Ref. [26] modeled an Economic Dispatch (ED) of multiple energy carriers considering wind energy (i.e. [27]) through a multi-agent genetic algorithm. This reference considered only one structure for all hubs with three forms of energy and without investigating a set of hubs which supply load. Also, in [26], the energy cost has been minimized only without considering the optimization of hub losses or a multi-objective problem (such as simultaneously minimizing the energy cost and losses of a set of hubs). In addition, some operational challenges such as valve-point loading effect and prohibited zones have not been taken into account.

1.1. Motivation, contribution, and novelty

ED in the power systems is a well-known problem and it is one of the most heavily used tools in the power system studies. It responses to schedule the committed outputs of all available generation units to meet the load demand at the minimum operating cost as well as satisfying different equality and inequality constraints [28]. The CHPED [29] is an extension version of the economic dispatch and can be considered as a special case of MCS problems in which two forms of energy, i.e. electricity and heat, are optimized simultaneously [6]. In the viewpoint of hub, the CHPED can be modeled with different hubs constructed by three elements including transformer (with 100% efficiency), CHP unit, and heater exchanger (with 100% efficiency). Fig. 1 shows this concept.

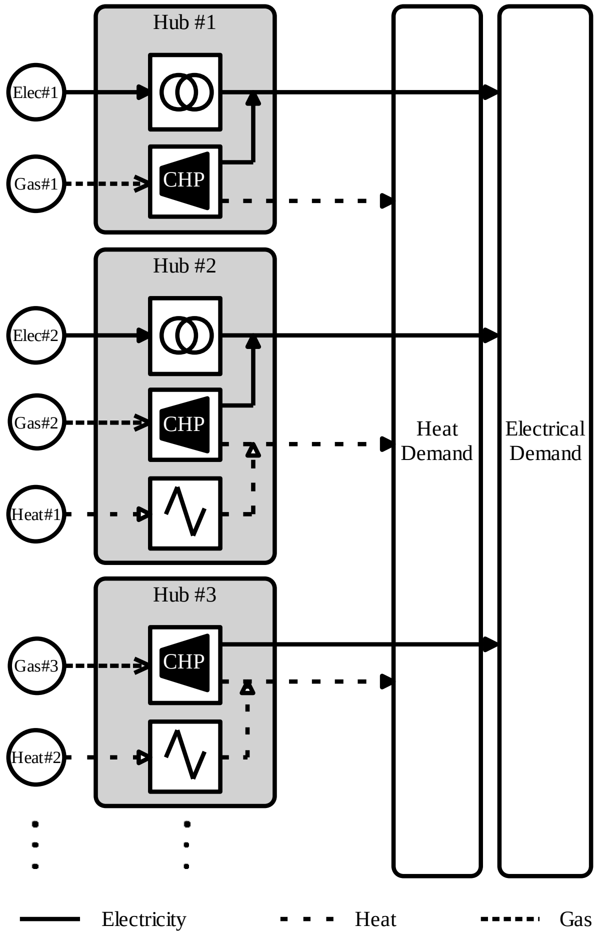

Fig. 1. A general representation of CHPED based on the hub concept

In this paper, motivation of CHPED modeling, based on the mentioned viewpoint, is extended to various hub structures with different converters and elements. So, an optimization framework is presented to formulate this new problem. It is mainly due to the fact that at this stage of the advancement of MCS, there is still needs to be put under examination in both modeling and operating concerns. Economic energy dispatch and conversion in the hubs are two main issues in the MCSs. In this condition, the classical ED methods should be modified to meet the system requirements like optimal conversion between different carriers.

The new proposed modeling, which is called Energy Hub Economic Dispatch (EHED), states a general economic representation covering a wide range of energies and hubs including different converters. This problem schedules the committed input carriers available at the hub inputs to meet different types of demands at minimum operating cost while satisfying various operational constraints. In other words, EHED allows finding an optimal operating point in terms of satisfying different equality and inequality constraints, supplying the various forms of load demands efficiently and economically, and searching the global optimum (or a less expensive solution) based on the objective function. Accordingly, three objective functions including energy cost of input carriers (as a single-objective), energy hub losses (as another single-objective), and a combination of them (as multi-objective) with different operational constraints are formulated to construct EHED problem. Therefore, the EHED problem is a nonlinear, non-convex, and high dimension one. It should be noted that to the best of authors' knowledge, none of the past researchers and publications have considered the mentioned extension with new futures to form the explained EHED problem.

In order to efficiently optimize the proposed optimization problem, a new modified version of Gravitational Search Algorithm (GSA), namely Self-Adaptive Learning with Time Varying Acceleration Coefficient GSA (SAL-TVAC-GSA), is suggested. The proposed algorithm is based on the Newtonian laws of gravitation and motion. In the suggested algorithm, three new strategies are considered to improve the performance of the original GSA and avoid trapping in local optima: 1) self-adaptive learning strategy; 2) considering time varying acceleration coefficient (a new strategy for *gbest*-guided); 3) a novel gravitational constant. The main feature of the proposed approach is due to its ability in solving quite large EHED problems yielding economical benefits with regard to the other tested algorithms. In fact, the suggested algorithm can search a better solution with a good convergence characteristic and a computational time fully compatible with operational planning time requirements. It should be noted that the contribution in this area derives from the capability of the suggested algorithm in being robust, i.e. always capable of finding a good quality solution without convergence problems and mostly yielding a better optimum which results in economical benefits which is our main performance indicator. Moreover, as long as authors know the proposed algorithm is a new optimization technique and has not been tested on this kind of problems before.

In summary, the main novelties and contribution of this work are:

- Proposing a general, simple, and suitable model for EHED in order to optimize various forms of energies as well as hub's conversions and flows. Furthermore, the energy hub-losses (instead of power losses only) are considered in the formulations. The presented formulation allows considering different carriers and taking into account the interactions between them.
- Covering different hubs with various structures. Different hub elements can be considered in the proposed model and each hub can be represented by a coupling matrix to demonstrate the interactions between various inputs and outputs. This subject is formulated as an equality constraint in EHED problem.
- Optimizing both single- and multi-objective EHED problems in terms of energy cost and hub losses. The hub losses are carried out as one of objectives in addition to the cost of various carriers.
- Considering the real-world conditions like valve-point loading effect and prohibited zones of electric-only units in formulations.
- Suggestion a new and powerful optimization algorithm, namely SAL-TVAC-GSA, to optimize the suggested EHED problem. The proposed optimization algorithm employs three fundamental modifications to enhance the quality solution and performance of the original GSA. The main characteristics and details of this new method can be found in section 4. Moreover, the obtained results demonstrate the ability and performance of the proposed optimization algorithm in finding a better quality solution than the other reported algorithms. Some advantages of the new algorithm are its simplicity of implementation, its accuracy, and its fast convergence to the optimal solution while satisfying all constraints.

- Demonstrating a new and complex test case to analyze the superior performance of the proposed optimization algorithm in terms of both solution accuracy and convergence performances.

1.2. Organization

The rest of this work is organized as follows: in section 2, the energy hub concept and the related general model as well as structures of the considered hubs are illustrated. In section 3, formulation of the proposed EHED problem in terms of different objective functions (both single- and multi-objective problems) and associated constraints is presented. Main structure of original GSA is described in section 4. Moreover, the suggested modifications applied to GSA to construct the proposed SAL-TVAC-GSA are presented in this section. Different steps of the suggested algorithm to solve EHED problem is described in section 5. The effectiveness of the proposed approach is verified by comparisons with various optimization algorithms such as TVAC-GSA, Enhanced GSA (EGSA), GSA, Particle Swarm Optimization (PSO), and Genetic Algorithm (GA) in Section 6. Finally, we will draw the conclusions.

2. Energy hub

2.1. Main structure

Generally, each energy hub makes an interface between delivered energy (by transmission networks and/or energy sources) and loads. In other words, various forms of energy (such as electricity, natural gas, etc.) are consumed at the input ports of a hub unit and different energy services (such as electricity, heat, coal, etc.) are provided at its output ports. This unit allows to integrate an arbitrary number of energy carriers and products [2]. Fig. 2 illustrates this concept. In this figure, the bidirectional arrow of conversion describes the energy flowing from input side to demand side and vice versa, e.g. electrical power flow through a transformer. However, for instance, in a gas turbine, energy only flows from input port to the output one.

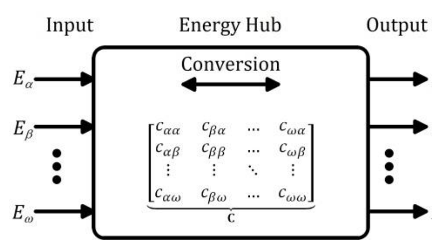

Fig. 2. A general and simple structure of an energy hub

The basic energy hub elements can be categorized as follows:

- Direct connection: this type delivers an input carrier to the output without converting it into another form or without significantly changing its quality (e.g., voltage and pressure). Electric cables, overhead lines, and pipelines are some examples in this regard.
- Converter: it transforms energy into a different form or quality such as steam and gas turbines, combustion engines, electric machines, and fuel cells.
- Storage devices: they store different forms of energy e.g. thermal storage capacity and electrical storage device.

Generally, the power plants (e.g. co- and tri-generations), industrial plants (e.g. refineries), big buildings (e.g. airports, hospitals, and shopping malls), and bounded geographical areas (e.g. cities) can be modeled as energy hubs. In this view point, an energy hub can be applied to any size of the modeled system [2,30] (e.g. at neighborhood scale [31]).

Converter elements or combinations of different converters in the form of energy hubs may have multiple in- and out-puts. Four types of conversions can be classified according to the number of in- and out-puts [2] as follows:

- Single Input and Single Output (SISO): the gas furnace is an example which converts natural gas to heat.
- Single Input and Multiple Output (SIMO): e.g. trigeneration which consumes natural gas and provides cool, heat, and electricity at output port.
- Multiple Input and Single Output (MISO): heat pump is an appropriate example which converts heat and electricity to heat.
- Multiple Input and Multiple Output (MIMO): an example of this type is reversible fuel cell which provides heat and electricity by consuming water and hydrogen [2].

A general MIMO model covering couplings can be formulated as follows [2]. According to (1), the mapping of input carriers to output ones of an energy hub can be modeled through a coupling matrix $\mathbf{C}$.

$$\underbrace{\begin{bmatrix} E_{\alpha}^{\text{out}} \\ E_{\beta}^{\text{out}} \\ \vdots \\ E_{\omega}^{\text{out}} \end{bmatrix}}_{\textbf{Output}} = \underbrace{\begin{bmatrix} c_{\alpha\alpha} & c_{\beta\alpha} & \cdots & c_{\omega\alpha} \\ c_{\alpha\beta} & c_{\beta\beta} & \cdots & c_{\omega\beta} \\ \vdots & \vdots & \ddots & \vdots \\ c_{\alpha\omega} & c_{\beta\omega} & \cdots & c_{\omega\omega} \end{bmatrix}}_{\mathbf{C}} \underbrace{\begin{bmatrix} E_{\alpha}^{\text{in}} \\ E_{\beta}^{\text{in}} \\ \vdots \\ E_{\omega}^{\text{in}} \end{bmatrix}}_{\textbf{Input}} \tag{1}$$

In (1), $\textbf{Input}$ denotes the vector of energy inputs; $\textbf{Output}$ is the energy outputs vector; $\mathbf{C}$ illustrates the coupling matrix; moreover, subscript $\{\alpha, \beta, \dots\}$ describes the energy carriers such as electricity, natural gas, etc.; and the entries of matrix $\mathbf{C}$ (i.e. $c_{\alpha\alpha}$, $c_{\alpha\beta}$, and etc.) are coupling factors.

Energy conversion in (1) is handled by coupling factors through relating an input to a certain output. Note that, as indicated in [2], in the simple cases such as transformers and gas furnaces, the coupling factor represents the steady state energy efficiency. Also, according to [2], in this paper, it is assumed that the coupling factors show constant efficiencies and so, the devices operate with constant efficiencies. In contrast, for a MIMO energy hub, the coupling factors are in general no longer equal to converter efficiencies. Since the received energy at input port may be split up to several converters, other coupling factors, namely *dispatch factors*, have to be considered. These factors define how energy flows from an input carrier are distributed among the hub elements. For a specific hub structure (see the following subsection) a similar conclusion can be considered for the output port. Therefore, in this paper, factors ν (or ν_1) is employed for input ports and also factor ν_2 is used for output port, if required. Therefore, each coupling factor contains " dispatch factor×converter efficiency" [2] (this concept will be employed in the next subsection). In this view point, the matrix $\mathbf{C}$ establishes a linear transformation because of the assumed constant efficiencies.

2.2. Different types of considered energy hubs

Main assumptions in this subsection are as follows:

- Within each energy hub, losses only occur in the convertor devices.
- Storage devices according to [2,32] can be included. But, it will not be considered explicitly here.
- Gross heating value is taken to be unit (for more details see [2]).

In this paper, 29 hub structures are investigated as illustrated in Fig. 3. In this figure, there are six elements as follows:

- Transformer: it delivers and provides electrical energy at its input and output, respectively.
- CHP: this device consumes the natural gas to produce electricity and heat.

- Combined Heat, Cool, and Power (CHCP): it converts the natural gas to electricity, heating, and cooling.
- Gas Furnace (GF): this device burns the natural gas and delivers heat.
- Heater Exchanger (HE): it consumes and provides heating at its input and output, respectively.
- Compressor air: this device products compressed air from electricity.

Based on these elements, five carriers including electricity, heat, cool, compressed air, as well as natural gas are denoted by subscripts e, h, c, a, and g, respectively. Energy conversion of the hubs presented in Fig. 3 can be stated as follows:

- Hub #1: this hub consists of only one transformer unit. The coupling matrix as well as the related input and output energy vectors can be represented as:

$$E_e^{\text{out}} = \begin{bmatrix} \overbrace{\eta_{\text{T}}}^{c_{ee}} \end{bmatrix} E_e^{\text{in}} \tag{2}$$

where η_{T} denotes the transformer efficiency.

- Hub #2: it contains only one CHP unit and is modeled as follows:

$$\begin{bmatrix} E_e^{\text{out}} \\ E_h^{\text{out}} \end{bmatrix} = \begin{bmatrix} \overbrace{\eta_{\text{CHP}_e}}^{c_{ge}} \\ \overbrace{\eta_{\text{CHP}_h}}^{c_{gh}} \end{bmatrix} E_g^{\text{in}} \tag{3}$$

where η_{CHP_e} and η_{CHP_h} are the electrical and heat efficiencies, respectively.

- Hub #3: a CHCP unit constructs this hub which can be represented as:

$$\begin{bmatrix} E_e^{\text{out}} \\ E_h^{\text{out}} \\ E_c^{\text{out}} \end{bmatrix} = \begin{bmatrix} \overbrace{\eta_{\text{CHCP}_e}}^{c_{ge}} \\ \overbrace{\eta_{\text{CHCP}_h}}^{c_{gh}} \\ \overbrace{\eta_{\text{CHCP}_c}}^{c_{gc}} \end{bmatrix} E_g^{\text{in}} \tag{4}$$

where η_{CHCP_e}, η_{CHCP_h}, and η_{CHCP_c} show the electrical, heat, and cool efficiencies of CHCP unit, respectively.

- Hub #4: this hub includes only one furnace and is formulated as:

$$E_h^{\text{out}} = \begin{bmatrix} \overbrace{\eta_{\text{GF}}}^{c_{gh}} \end{bmatrix} E_g^{\text{in}} \tag{5}$$

where the furnace's efficiency is denoted by η_{GF}.

- Hub #5: one heater exchanger is the main structure of this hub and can be stated as follows:

$$E_h^{\text{out}} = \begin{bmatrix} \overbrace{\eta_{\text{HE}}}^{c_{hh}} \end{bmatrix} E_h^{\text{in}} \tag{6}$$

where η_{HE} is the HE's efficiency.

- Hub #6: the electricity and gas are consumed by transformer and CHP unit located in this hub to provide electricity and heating at the output through the following mathematical configuration:

$$\begin{bmatrix} E_e^{\text{out}} \\ E_h^{\text{out}} \end{bmatrix} = \begin{bmatrix} \overbrace{\eta_{\text{T}}}^{c_{ee}} & \overbrace{\eta_{\text{CHP}_e}}^{c_{ge}} \\ \overbrace{0}^{c_{eh}} & \overbrace{\eta_{\text{CHP}_h}}^{c_{gh}} \end{bmatrix} \begin{bmatrix} E_e^{\text{in}} \\ E_g^{\text{in}} \end{bmatrix} \tag{7}$$

- Hub #7: this hub produces electricity, heating as well as compressed air by employing the electrical energy, as follows:

$$\begin{bmatrix} E_e^{\text{out}} \\ E_h^{\text{out}} \\ E_a^{\text{out}} \end{bmatrix} = \begin{bmatrix} \overbrace{(1-\nu)\eta_{\text{T}}}^{c_{ee}} \\ \overbrace{\nu\eta_{\text{C}_h}\eta_{\text{T}}}^{c_{eh}} \\ \overbrace{\nu\eta_{\text{C}_a}\eta_{\text{T}}}^{c_{ea}} \end{bmatrix} E_e^{\text{in}} \tag{8}$$

where η_{C_h} and η_{C_a} are compressor air's efficiencies related to the heat and air, respectively.

- Hub #8: electricity, heating, and cooling can be provided by this hub through consuming the electrical and gas energies as follows:

$$\begin{bmatrix} E_e^{\text{out}} \\ E_h^{\text{out}} \\ E_c^{\text{out}} \end{bmatrix} = \begin{bmatrix} \overbrace{\eta_{\text{T}}}^{c_{ee}} & \overbrace{\eta_{\text{CHCP}_e}}^{c_{ge}} \\ \overbrace{0}^{c_{eh}} & \overbrace{\eta_{\text{CHCP}_h}}^{c_{gh}} \\ \overbrace{0}^{c_{ec}} & \overbrace{\eta_{\text{CHCP}_c}}^{c_{gc}} \end{bmatrix} \begin{bmatrix} E_e^{\text{in}} \\ E_g^{\text{in}} \end{bmatrix} \tag{9}$$

- Hub #9: one CHP unit and one gas furnace convert the dispatched natural gas into the electricity and heating through the following formula:

$$\begin{bmatrix} E_e^{\text{out}} \\ E_h^{\text{out}} \end{bmatrix} = \begin{bmatrix} \overbrace{\nu\eta_{\text{CHP}_e}}^{c_{ge}} \\ \overbrace{\nu\eta_{\text{CHP}_h} + (1-\nu)\eta_{\text{GF}}}^{c_{gh}} \end{bmatrix} E_g^{\text{in}} \tag{10}$$

- Hub #10: two forms of energy including heating and gas at the hub input, are converted to electrical energy and heating for customers as follows:

$$\begin{bmatrix} E_e^{\text{out}} \\ E_h^{\text{out}} \end{bmatrix} = \begin{bmatrix} \overbrace{\eta_{\text{CHP}_e}}^{c_{ge}} & \overbrace{0}^{c_{he}} \\ \overbrace{\eta_{\text{CHP}_h}}^{c_{gh}} & \overbrace{\eta_{\text{HE}}}^{c_{hh}} \end{bmatrix} \begin{bmatrix} E_g^{\text{in}} \\ E_h^{\text{in}} \end{bmatrix} \tag{11}$$

- Hub #11: this hub is constructed by employing and CHCP units and described as:

$$\begin{bmatrix} E_e^{\text{out}} \\ E_h^{\text{out}} \\ E_c^{\text{out}} \end{bmatrix} = \begin{bmatrix} \overbrace{\eta_{\text{CHCP}_e}}^{c_{ge}} & \overbrace{0}^{c_{he}} \\ \overbrace{\eta_{\text{CHCP}_h}}^{c_{gh}} & \overbrace{\eta_{\text{HE}}}^{c_{hh}} \\ \overbrace{\eta_{\text{CHCP}_c}}^{c_{gc}} & \overbrace{0}^{c_{hc}} \end{bmatrix} \begin{bmatrix} E_g^{\text{in}} \\ E_h^{\text{in}} \end{bmatrix} \tag{12}$$

- Hub #12: it provides heating, cooling, and electricity by using the natural gas based on the following representation:

$$\begin{bmatrix} E_e^{\text{out}} \\ E_h^{\text{out}} \\ E_c^{\text{out}} \end{bmatrix} = \begin{bmatrix} \overbrace{\nu\eta_{\text{CHCP}_e}}^{c_{ge}} \\ \overbrace{\nu\eta_{\text{CHCP}_h} + (1-\nu)\eta_{\text{GF}}}^{c_{gh}} \\ \overbrace{\nu\eta_{\text{CHCP}_c}}^{c_{gc}} \end{bmatrix} E_g^{\text{in}} \tag{13}$$

- Hub #13: this hub delivers two input carriers (i.e. electricity and heating) to the output without converting them into another form of energy as follows:

$$\begin{bmatrix} E_e^{\text{out}} \\ E_h^{\text{out}} \end{bmatrix} = \begin{bmatrix} \overbrace{\eta_{\text{T}}}^{c_{ee}} & \overbrace{0}^{c_{he}} \\ \overbrace{0}^{c_{eh}} & \overbrace{\eta_{\text{HE}}}^{c_{hh}} \end{bmatrix} \begin{bmatrix} E_e^{\text{in}} \\ E_h^{\text{in}} \end{bmatrix} \tag{14}$$

- Hub #14: transformer and GF provide electrical and heating energies for loads as:

$$\begin{bmatrix} E_e^{\text{out}} \\ E_h^{\text{out}} \end{bmatrix} = \begin{bmatrix} \overbrace{\eta_{\text{T}}}^{c_{ee}} & \overbrace{0}^{c_{ge}} \\ \overbrace{0}^{c_{eh}} & \overbrace{\eta_{\text{GF}}}^{c_{gh}} \end{bmatrix} \begin{bmatrix} E_e^{\text{in}} \\ E_g^{\text{in}} \end{bmatrix} \tag{15}$$

- Hub #15: in this hub, two forms of energies, i.e. heating and gas, are converted to heating as below:

$$E_h^{\text{out}} = \begin{bmatrix} \overbrace{\eta_{\text{GF}}}^{c_{gh}} & \overbrace{\eta_{\text{HE}}}^{c_{hh}} \end{bmatrix} \begin{bmatrix} E_g^{\text{in}} \\ E_h^{\text{in}} \end{bmatrix} \tag{16}$$

- Hub #16: delivering four forms of energy including electricity, heating, cooling, and compressed air by employing only the natural gas is performed through this hub through as following:

$$\begin{bmatrix} E_e^{\text{out}} \\ E_h^{\text{out}} \\ E_c^{\text{out}} \\ E_a^{\text{out}} \end{bmatrix} = \begin{bmatrix} \overbrace{(1-\nu)\eta_{\text{CHCP}_e}}^{c_{ge}} \\ \overbrace{\eta_{\text{CHCP}_h} + \nu\eta_{\text{CHCP}_e}\eta_{\text{C}_h}}^{c_{gh}} \\ \overbrace{\eta_{\text{CHCP}_c}}^{c_{gc}} \\ \overbrace{\nu\eta_{\text{CHCP}_e}\eta_{\text{C}_a}}^{c_{ga}} \end{bmatrix} E_g^{\text{in}} \tag{17}$$

- Hub #17: it is similar to previous structure; but, CHCP unit has been replaced by a CHP. Mathematical representation of this hub, which provides three carriers (i.e. electricity, heating, and compressed air) from the natural gas, is as follows:

$$\begin{bmatrix} E_e^{\text{out}} \\ E_h^{\text{out}} \\ E_a^{\text{out}} \end{bmatrix} = \begin{bmatrix} \overbrace{(1-\nu)\eta_{\text{CHP}_e}}^{c_{ge}} \\ \overbrace{\eta_{\text{CHP}_h} + \nu\eta_{\text{CHP}_e}\eta_{\text{C}_h}}^{c_{gh}} \\ \overbrace{\nu\eta_{\text{CHP}_e}\eta_{\text{C}_a}}^{c_{ga}} \end{bmatrix} E_g^{\text{in}} \tag{18}$$

- Hub #18: this hub consists of three elements (i.e. transformer, CHCP, and HE) to convert electricity, gas, and heat into electricity, heating, and cooling as below:

$$\begin{bmatrix} E_e^{\text{out}} \\ E_h^{\text{out}} \\ E_a^{\text{out}} \end{bmatrix} = \begin{bmatrix} \overbrace{\eta_T}^{c_{ee}} & \overbrace{\eta_{\text{CHCP}_e}}^{c_{ge}} & \overbrace{0}^{c_{he}} \\ \overbrace{0}^{c_{eh}} & \overbrace{\eta_{\text{CHCP}_h}}^{c_{gh}} & \overbrace{\eta_{\text{HE}}}^{c_{hh}} \\ \overbrace{0}^{c_{ea}} & \overbrace{\eta_{\text{CHCP}_c}}^{c_{ga}} & \overbrace{0}^{c_{ha}} \end{bmatrix} \begin{bmatrix} E_e^{\text{in}} \\ E_g^{\text{in}} \\ E_h^{\text{in}} \end{bmatrix} \tag{19}$$

- Hub #19: heater exchanger, CHP, and transformer construct this hub to deliver heating and electrical energy through consuming and converting electricity, gas, and heating as follows:

$$\begin{bmatrix} E_e^{\text{out}} \\ E_h^{\text{out}} \end{bmatrix} = \begin{bmatrix} \overbrace{\eta_{\text{T}}}^{c_{ee}} & \overbrace{\eta_{\text{CHP}_e}}^{c_{ge}} & \overbrace{0}^{c_{he}} \\ \overbrace{0}^{c_{eh}} & \overbrace{\eta_{\text{CHP}_h}}^{c_{gh}} & \overbrace{\eta_{\text{HE}}}^{c_{hh}} \end{bmatrix} \begin{bmatrix} E_e^{\text{in}} \\ E_g^{\text{in}} \\ E_h^{\text{in}} \end{bmatrix} \tag{20}$$

- Hub #20: in this hub, three elements including transformer, CHP, and gas furnace, convert electricity and gas into electricity and heating as follows:

$$\begin{bmatrix} E_e^{\text{out}} \\ E_h^{\text{out}} \end{bmatrix} = \begin{bmatrix} \overbrace{\eta_{\text{T}}}^{c_{ee}} & \overbrace{\nu\eta_{\text{CHP}_e}}^{c_{ge}} \\ \overbrace{0}^{c_{eh}} & \overbrace{\nu\eta_{\text{CHP}_h} + (1-\nu)\eta_{\text{GF}}}^{c_{gh}} \end{bmatrix} \begin{bmatrix} E_e^{\text{in}} \\ E_g^{\text{in}} \end{bmatrix} \tag{21}$$

- Hub #21: it employs CHCP, furnace, and transformer through the following mathematical configuration.

$$\begin{bmatrix} E_e^{\text{out}} \\ E_h^{\text{out}} \\ E_c^{\text{out}} \end{bmatrix} = \begin{bmatrix} \overbrace{\eta_{\text{T}}}^{c_{ee}} & \overbrace{\nu\eta_{\text{CHCP}_e}}^{c_{ge}} \\ \overbrace{0}^{c_{eh}} & \overbrace{\nu\eta_{\text{CHCP}_h} + (1-\nu)\eta_{\text{GF}}}^{c_{gh}} \\ \overbrace{0}^{c_{ec}} & \overbrace{\nu\eta_{\text{CHCP}_c}}^{c_{gc}} \end{bmatrix} \begin{bmatrix} E_e^{\text{in}} \\ E_g^{\text{in}} \end{bmatrix} \tag{22}$$

- Hub #22: transformer, CHCP, and compressor air convert electricity and heating into electricity, heating, cooling, and compressed air through the following conversion.

$$\begin{bmatrix} E_e^{\text{out}} \\ E_h^{\text{out}} \\ E_c^{\text{out}} \\ E_a^{\text{out}} \end{bmatrix} = \begin{bmatrix} \overbrace{(1-\nu)\eta_{\text{T}}}^{c_{ee}} & \overbrace{(1-\nu)\eta_{\text{CHCP}_e}}^{c_{ge}} \\ \overbrace{\nu\eta_{\text{T}}\eta_{\text{C}_h}}^{c_{eh}} & \overbrace{\eta_{\text{CHCP}_h} + \nu\eta_{\text{CHCP}_e}\eta_{\text{C}_h}}^{c_{gh}} \\ \overbrace{0}^{c_{ec}} & \overbrace{\eta_{\text{CHCP}_c}}^{c_{gc}} \\ \overbrace{\nu\eta_{\text{T}}\eta_{\text{C}_a}}^{c_{ea}} & \overbrace{\nu\eta_{\text{CHCP}_e}\eta_{\text{C}_a}}^{c_{ga}} \end{bmatrix} \begin{bmatrix} E_e^{\text{in}} \\ E_g^{\text{in}} \end{bmatrix} \tag{23}$$

- Hub #23: this hub equipped with transformer, CHP, and compressor air as:

$$\begin{bmatrix} E_e^{\text{out}} \\ E_h^{\text{out}} \\ E_a^{\text{out}} \end{bmatrix} = \begin{bmatrix} \overbrace{(1-\nu)\eta_{\text{T}}}^{c_{ee}} & \overbrace{(1-\nu)\eta_{\text{CHP}_e}}^{c_{ge}} \\ \overbrace{\nu\eta_{\text{T}}\eta_{\text{C}_h}}^{c_{eh}} & \overbrace{\eta_{\text{CHP}_h} + \nu\eta_{\text{CHP}_e}\eta_{\text{C}_h}}^{c_{gh}} \\ \overbrace{\nu\eta_{\text{T}}\eta_{\text{C}_a}}^{c_{ea}} & \overbrace{\nu\eta_{\text{CHP}_e}\eta_{\text{C}_a}}^{c_{ga}} \end{bmatrix} \begin{bmatrix} E_e^{\text{in}} \\ E_g^{\text{in}} \end{bmatrix} \tag{24}$$

- Hub #24: four elements including transformer, CHCP, gas furnace, and compressor air deliver four types of carriers (i.e. electricity, heating, cooling, and compressed air) by using two forms of energy consisting of electrical and gas as below:

$$\begin{bmatrix} E_e^{\text{out}} \\ E_h^{\text{out}} \\ E_c^{\text{out}} \\ E_a^{\text{out}} \end{bmatrix} = \begin{bmatrix} \overbrace{(1-\nu_2)\eta_{\text{T}}}^{c_{ee}} & \overbrace{\nu_1(1-\nu_2)\eta_{\text{CHCP}_e}}^{c_{ge}} \\ \overbrace{\nu_2\eta_{\text{T}}\eta_{\text{C}_h}}^{c_{eh}} & \overbrace{\nu_1\eta_{\text{CHCP}_h} + (1-\nu_1)\eta_{\text{GF}} + \nu_1\nu_2\eta_{\text{CHCP}_e}\eta_{\text{C}_h}}^{c_{gh}} \\ \overbrace{0}^{c_{ec}} & \overbrace{\nu_1\eta_{\text{CHCP}_c}}^{c_{gc}} \\ \overbrace{\nu_2\eta_{\text{T}}\eta_{\text{C}_a}}^{c_{ea}} & \overbrace{\nu_1\nu_2\eta_{\text{CHCP}_e}\eta_{\text{C}_a}}^{c_{ga}} \end{bmatrix} \begin{bmatrix} E_e^{\text{in}} \\ E_g^{\text{in}} \end{bmatrix} \tag{25}$$

- Hub #25: the structure of this hub is as previous hub; but, CHCP unit has been replaced by a CHP one. So, the energy conversion can be formulated as follows:

$$\begin{bmatrix} E_e^{\text{out}} \\ E_h^{\text{out}} \\ E_a^{\text{out}} \end{bmatrix} = \begin{bmatrix} \overbrace{(1-\nu_2)\eta_{\text{T}}}^{c_{ee}} & \overbrace{\nu_1(1-\nu_2)\eta_{\text{CHP}_e}}^{c_{ge}} \\ \overbrace{\nu_2\eta_{\text{T}}\eta_{\text{C}_h}}^{c_{eh}} & \overbrace{\nu_1\eta_{\text{CHP}_h} + (1-\nu_1)\eta_{\text{GF}} + \nu_1\nu_2\eta_{\text{CHP}_e}\eta_{\text{C}_h}}^{c_{gh}} \\ \overbrace{\nu_2\eta_{\text{T}}\eta_{\text{C}_a}}^{c_{ea}} & \overbrace{\nu_1\nu_2\eta_{\text{CHP}_e}\eta_{\text{C}_a}}^{c_{ga}} \end{bmatrix} \begin{bmatrix} E_e^{\text{in}} \\ E_g^{\text{in}} \end{bmatrix} \tag{26}$$

- Hub #26: it transforms electricity, gas, and heating into electricity, heating, cooling, and compressed air through transformer, CHCP, HE, and compressor air as below:

$$\begin{bmatrix} E_e^{\text{out}} \\ E_h^{\text{out}} \\ E_c^{\text{out}} \\ E_a^{\text{out}} \end{bmatrix} = \begin{bmatrix} \overbrace{(1-\nu)\eta_{\text{T}}}^{c_{ee}} & \overbrace{(1-\nu)\eta_{\text{CHCP}_e}}^{c_{ge}} & \overbrace{0}^{c_{he}} \\ \overbrace{\nu\eta_{\text{T}}\eta_{\text{C}_h}}^{c_{eh}} & \overbrace{\eta_{\text{CHCP}_h} + \nu\eta_{\text{CHCP}_e}\eta_{\text{C}_h}}^{c_{gh}} & \overbrace{\eta_{\text{HE}}}^{c_{hh}} \\ \overbrace{0}^{c_{ec}} & \overbrace{\eta_{\text{CHCP}_c}}^{c_{gc}} & \overbrace{0}^{c_{hc}} \\ \overbrace{\nu\eta_{\text{T}}\eta_{\text{C}_a}}^{c_{ea}} & \overbrace{\nu\eta_{\text{CHCP}_e}\eta_{\text{C}_a}}^{c_{ga}} & \overbrace{0}^{c_{ha}} \end{bmatrix} \begin{bmatrix} E_e^{\text{in}} \\ E_g^{\text{in}} \\ E_h^{\text{in}} \end{bmatrix} \tag{27}$$

- Hub #27: electricity, gas, and heating are converted into electricity, heating, and compressed air by this hub equipped with transformer, HE, CHP, and compressor air. The mathematical representation of this energy conversion can be stated as:

$$\begin{bmatrix} E_e^{\text{out}} \\ E_h^{\text{out}} \\ E_a^{\text{out}} \end{bmatrix} = \begin{bmatrix} \overbrace{(1-\nu)\eta_{\text{T}}}^{c_{ee}} & \overbrace{(1-\nu)\eta_{\text{CHP}_e}}^{c_{ge}} & \overbrace{0}^{c_{he}} \\ \overbrace{\nu\eta_{\text{T}}\eta_{\text{C}_h}}^{c_{eh}} & \overbrace{\eta_{\text{CHP}_h} + \nu\eta_{\text{CHP}_e}\eta_{\text{C}_h}}^{c_{gh}} & \overbrace{\eta_{\text{HE}}}^{c_{hh}} \\ \overbrace{\nu\eta_{\text{T}}\eta_{\text{C}_a}}^{c_{ea}} & \overbrace{\nu\eta_{\text{CHP}_e}\eta_{\text{C}_a}}^{c_{ga}} & \overbrace{0}^{c_{ha}} \end{bmatrix} \begin{bmatrix} E_e^{\text{in}} \\ E_g^{\text{in}} \\ E_h^{\text{in}} \end{bmatrix} \tag{28}$$

- Hub #28: it consists of five converters (i.e. transformer, CHCP, heater exchanger, gas furnace, and compressor air) to supply electrical, heat, cool, and compressed air demands by consuming electricity, gas, and heating as follows:

$$\begin{bmatrix}E_e^{\text{out}}\\E_h^{\text{out}}\\E_c^{\text{out}}\\E_a^{\text{out}}\end{bmatrix} = \begin{bmatrix} \overbrace{(1-\nu_2)\eta_{\text{T}}}^{c_{ee}} & \overbrace{\nu_1(1-\nu_2)\eta_{\text{CHCP}_e}}^{c_{ge}} & \overbrace{0}^{c_{he}} \\ \overbrace{\nu_2\eta_{\text{T}}\eta_{\text{C}_h}}^{c_{eh}} & \overbrace{\nu_1\eta_{\text{CHCP}_h}+(1-\nu_1)\eta_{\text{GF}}+\nu_1\nu_2\eta_{\text{CHCP}_e}\eta_{\text{C}_h}}^{c_{gh}} & \overbrace{\eta_{\text{HE}}}^{c_{hh}} \\ \overbrace{0}^{c_{ec}} & \overbrace{\nu_1\eta_{\text{CHCP}_c}}^{c_{gc}} & \overbrace{0}^{c_{hc}} \\ \overbrace{\nu_2\eta_{\text{T}}\eta_{\text{C}_a}}^{c_{ea}} & \overbrace{\nu_1\nu_2\eta_{\text{CHCP}_e}\eta_{\text{C}_a}}^{c_{ga}} & \overbrace{0}^{c_{ha}}\end{bmatrix}\begin{bmatrix}E_e^{\text{in}}\\E_g^{\text{in}}\\E_h^{\text{in}}\end{bmatrix} \tag{29}$$

- Hub #29: it uses transformer, CHP, GF, HE, and compressor air in order to transform electricity, gas, and heating into electricity, heating, and compressed air. The mathematical configuration of this hub can be represented as follows:

$$\begin{bmatrix}E_e^{\text{out}}\\E_h^{\text{out}}\\E_a^{\text{out}}\end{bmatrix} = \begin{bmatrix} \overbrace{(1-\nu_2)\eta_{\text{T}}}^{c_{ee}} & \overbrace{\nu_1(1-\nu_2)\eta_{\text{CHP}_e}}^{c_{ge}} & \overbrace{0}^{c_{he}} \\ \overbrace{\nu_2\eta_{\text{T}}\eta_{\text{C}_h}}^{c_{eh}} & \overbrace{\nu_1\eta_{\text{CHP}_h}+(1-\nu_1)\eta_{\text{GF}}+\nu_1\nu_2\eta_{\text{CHP}_e}\eta_{\text{C}_h}}^{c_{gh}} & \overbrace{\eta_{\text{HE}}}^{c_{hh}} \\ \overbrace{\nu_2\eta_{\text{T}}\eta_{\text{C}_a}}^{c_{ea}} & \overbrace{\nu_1\nu_2\eta_{\text{CHP}_e}\eta_{\text{C}_h}}^{c_{ga}} & \overbrace{0}^{c_{ha}}\end{bmatrix}\begin{bmatrix}E_e^{\text{in}}\\E_g^{\text{in}}\\E_h^{\text{in}}\end{bmatrix} \tag{30}$$

Note that, the hub’s structures presented in this subsection denote some related structures and do not cover all possible configurations which can be made by transformer, CHP, CHCP, GF, HE, and compressor. Also, considering other hub elements can extend this list.

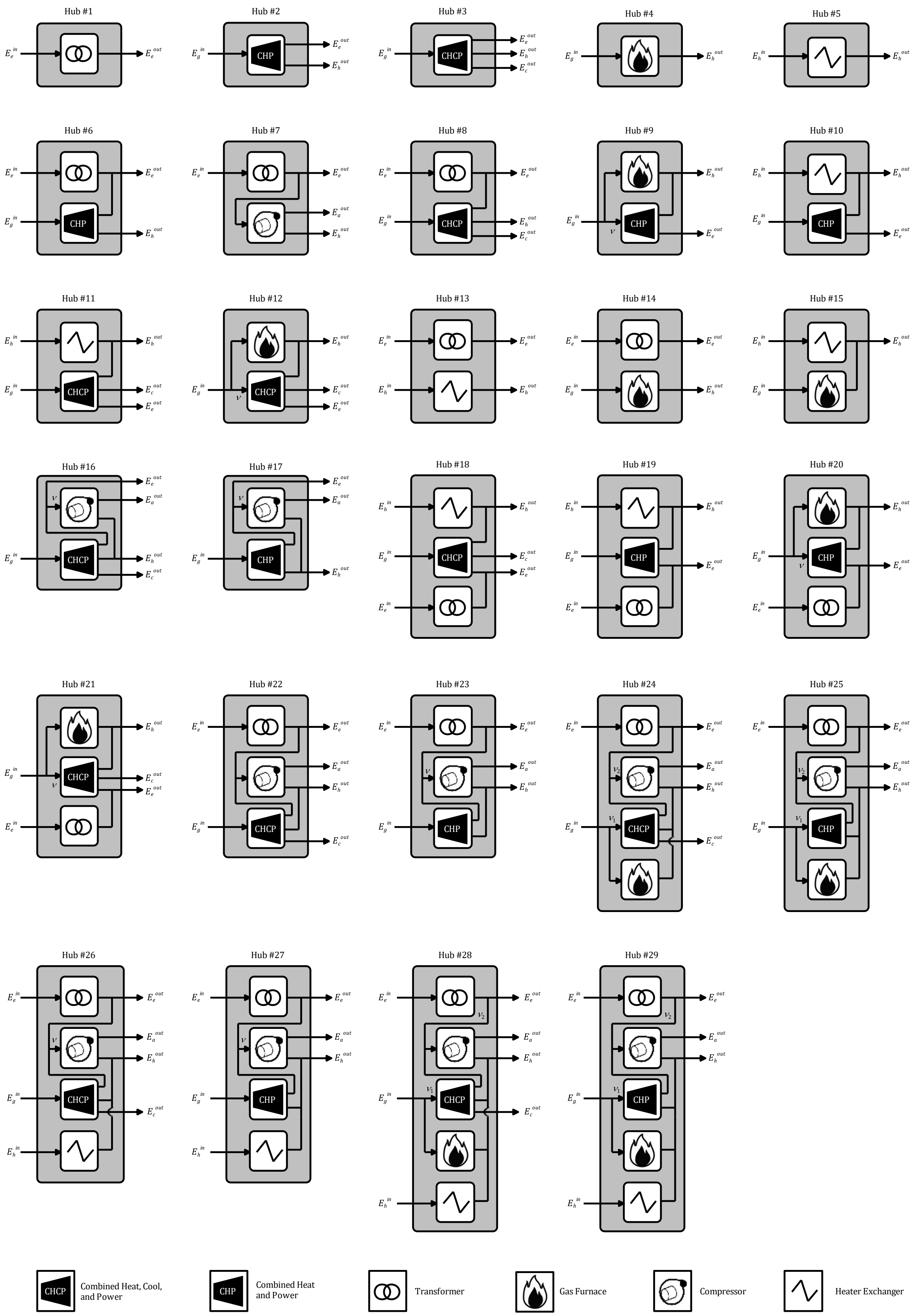

Fig. 3. The hub structures considered in this paper.

3. EHED problem

The problem formulation related to EHED can be stated as an objective function which to be minimized subject to satisfy all equality and inequality constraints. So, in this section, objective function and main constraints are presented.

3.1. Objective function

In this paper, three objective functions are considered as:

1) Energy cost minimization (single-objective problem): the energy production cost of all available carriers (i.e. electricity, natural gas, and heating) at the hub input is optimized as (31). The energy carriers offered at the input can be seen as energy generators with different cost structures [33]. Note that, considering the valve-point loading effect increases the complexity of the objective function and make it non-smooth and non-convex. Multi-valve steam turbines in large steam turbine generators produced a rippling effect on the input-output characteristic which known as "valve-point loading effect" [6]. Thus the generating unit output is not always smooth as shown in Fig. 4.

$$OF_1 = \sum_{i\in\{g,h\}} \sum_{j=1}^{n_i} \left(a_{j,i} + b_{j,i}E_{j,i}^{\text{in}} + c_{j,i}\left(E_{j,i}^{\text{in}}\right)^2\right) + \sum_{j=1}^{n_e} \left(a_{j,e} + b_{j,e}E_{j,e}^{\text{in}} + c_{j,e}\left(E_{j,e}^{\text{in}}\right)^2 + \left|d_{j,e}\sin\left(e_{j,e}\left(E_{j,e}^{\text{in,min}} - E_{j,e}^{\text{in}}\right)\right)\right|\right) \quad (31)$$

where $\{a_{j,i}, b_{j,i}, c_{j,i}\}$ are cost coefficients of jth source (energy offered at input has been modeled as energy sources) related to ith input carrier; also, $e_{j,e}$ and $d_{j,e}$ are the cost coefficients for modeling valve-point effect for electrical carrier; n_i denotes the total number of energy sources associated with ith input carrier; $E_{j,i}^{\text{in}}$ represents the energy production of jth source and ith input carrier; and finally, OF denotes the objective function.

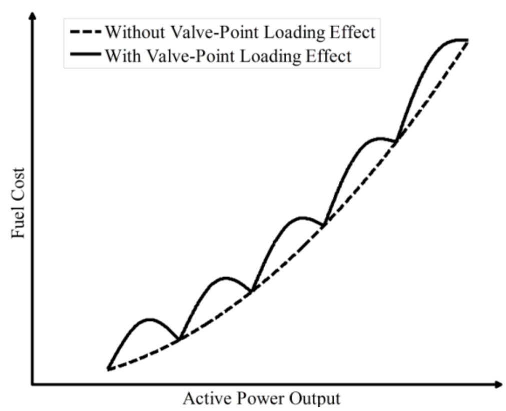

Fig. 4. Fuel cost curve with/without valve-point loading effect [6].

2) Minimization of energy hub losses (single-objective problem): this objective deals with minimizing the overall energy losses for all carriers which occurs in all energy hubs. This function reduces the differences between the total input and output energies in all hubs as follows:

$$OF_2 = \sum_{i \in \{e,g,h\}} \sum_{j=1}^{N_{hub}} \left(E_{j,i}^{\text{in}} - E_i^{\text{demand}} \right) \tag{32}$$

where E_i^{demand} represents the energy demand of the systems for output carrier i; and N_{hub} denotes the total number of hubs.

3) Minimization of energy cost and hub losses: applying the formulation presented in [16,34], a multi-objective problem can be converted to a single-objective problem as follows:

$$OF_3 = OF_1 \left(1 + \frac{OF_2}{\sum_{i \in \{e,g,h\}} E_i^{\text{demand}}} \right) \tag{33}$$

3.2. Constraints

The mentioned optimization problem should be minimized subject to the following constraints:

- Energy flow equation in energy hubs (balance equation of hubs): the general formula (1), which was illustrated in (2)–(30) for different hub structures, shuold be met as below for all hubs in a system:

$$\mathbf{Input}_i = \mathbf{C}_i \mathbf{Output}_i, \;\; i = 1, \dots, N_{hub} \tag{34}$$

- Energy output of hubs and demand balance: following constraint should be satisfied regarding to all hub's output carriers:

$$\sum_{j=1}^{N_{hub}} E_{j,i}^{\text{out}} = E_i^{\text{demand}}, \;\; i \in \{e, h, c, a\} \tag{35}$$

  Note that, $E_{j,i}^{\text{out}} = 0$ if jth hub does not have ith form of energy at its output.

- Capacity limits of all energy units (limitations on hub inputs): for all connected units (heat-only, gas-only, and electric-only ones) to the hubs, following inequality constraint should be investigated:

$$E_{j,i}^{\text{in,min}} \le E_{j,i}^{\text{in}} \le E_{j,i}^{\text{in,max}}, \;\; i \in \{e, g, h\} \text{ and } j = 1, \dots, n_i \tag{36}$$

  In this paper, prohibited operating zones are considered for some electric-only units (conventional thermal ones) [35]. This effect could be mainly due to vibration in the shaft bearing caused by the steam valve or faults in the machines themselves or the associated auxiliary equipment, such as boilers and feed pumps [35]. In this condition, the best economy will be achieved when operation in these zones will be avoided. So, prohibited operating zones create disjoint feasible sub-regions and make a non-continuous problem. Hence, the feasible operation of such units can be expressed as follows:

$$\begin{gathered} E_{j,e}^{\text{in,min}} \le E_{j,e}^{\text{in}} \le E_{j,e}^{\text{in,min}_{z_1}} \\ E_{j,e}^{\text{in,max}_{z_1}} \le E_{j,e}^{\text{in}} \le E_{j,e}^{\text{in,min}_{z_2}} \\ E_{j,e}^{\text{in,max}_{z_{i-1}}} \le E_{j,e}^{\text{in}} \le E_{j,e}^{\text{in,max}}, \;\; i = 1, \dots, n_{zone_j}, \\ j \in \{\text{Electric units with prohibited zones}\} \end{gathered} \tag{37}$$

  where n_{zone_j} denotes the number of prohibited zones of the jth electrical unit; $\min_{z_i}$ and $\max_{z_i}$ are upper and lower bounds on zone ith, respectively.

- Dispatch factor limitation of energy hubs: all dispatch factors related to input or output ports should satisfy the following inequality constraint:

$$0 \leq \nu \leq 1 \tag{38}$$

4. SAL-TVAC-GSA structure

4.1. Original GSA structure

Firstly, Rashedi et al. [36] in 2009 proposed the GSA based on the gravitational law and laws of motion between masses (Newtonian laws). This technique is capable of handling large-scale nonlinear and non-convex problems as demonstrated in literature [6,34,36–39]. In order to fully understand how this algorithm works, its structure can be represented in the following.

Suppose that there are N masses (as N agents) and the position of each mass corresponds to a potential solution of the problem. Therefore, the position of the ith mass can be defined as follows:

$$X_i = \left[x_i^1, \dots, x_i^d, \dots, x_i^n\right]^T \quad i = 1, 2, \dots, N \tag{39}$$

where x_i^d represents the position of the ith mass in the dth dimension. $(\cdot)^T$ denotes the transposition of $(\cdot)$.

Gravity exists everywhere and every particle in the universe attracts the other particles (Fig. 5). The gravitational force between two particles is inversely proportional to the square of the distance between them and directly proportional to the product of their masses. Therefore, the gravitational force between heavier masses with short distance is the highest. Therefore, based on the law of gravity, each mass attracts every other mass and the gravitational force between the ith mass because of the jth mass in dth dimension at specific time t is as (40). This is because of the fact that the gravity acts between separated particles without any intermediary and delay [36].

$$F_{ij}^d = G(t) \times \frac{M_i(t) M_j(t)}{R_{ij}(t) + \varepsilon} \times \left(x_j^d(t) - x_i^d(t)\right) \tag{40}$$

with

$$G(t) = G_0 \exp\left(\frac{-\delta t}{\text{Iteration}_{\max}}\right) \tag{41}$$

$$R_{ij}(t) = \left\| X_i(t), X_j(t) \right\|_2 \tag{42}$$

and where $G(t)$ is the gravitational constant which is reduced with time (iteration, age of universe) to control search accuracy [36]. G_0 is the initial value of $G(t)$; $\text{Iteration}_{\max}$ represents the maximum number of iterations; δ is a constant term; $R_{ij}(t)$ denotes the Euclidian distance between ith and jth mass; it is essential to note that according to [6,16,34,36], $R_{ij}(t)$ provides better performance than $R_{ij}^2(t)$ unlike the law of gravity between two particles.

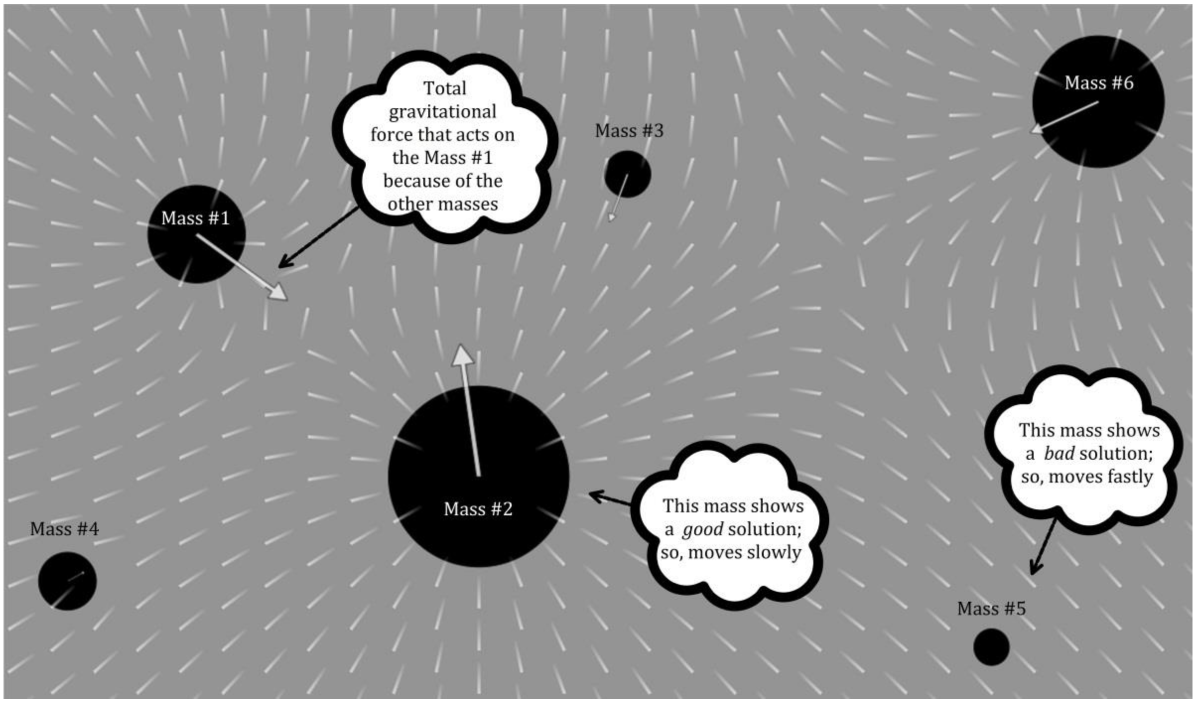

Fig. 5. The concept of the gravitational force between masses.

The total gravitational force that acts on the ith mass in the dth dimension is a randomly weighted sum of dth components of the forces exerted from other masses as (43).

$$F_i^d(t) = \sum_{\substack{j=1 \\ j \neq i}}^{N} \mathrm{rand}_j \times F_{ij}^d(t) \tag{43}$$

where rand_j denotes a random number in the interval $[0, 1]$.

At the beginning of the optimization process, the reduction of the number of masses with lapse of time in (43) allows the exploration of the space of solutions to avoid trapping in a local optimum. Also, the exploitation power fades with lapse of time. So, a set of agents with heavier masses (K_{best} agents corresponding to good solutions) only apply their gravitational force to the other [36]. K_{best} with initial value K_0 is a function of time which is reduced with the iteration linearly. So, the performance of GSA will be improved by modifying (43) as (44).

$$F_i^d(t) = \sum_{\substack{j \in K_{\mathrm{best}} \\ j \neq i}}^{N} \mathrm{rand}_j \times F_{ij}^d(t) \tag{44}$$

where K_0 is a first set of masses with the best fitness value and heaviest mass which denotes the K_{best}.

The acceleration $a_i^d(t)$ of the ith mass at time t in dimension d, according to the Newton's law of motion is as:

$$a_i^d(t) = \frac{F_i^d(t)}{M_{ii}(t)} \tag{45}$$

where M_{ii} represents the inertial mass of the ith agent. Inertial mass denotes the resistance of a mass to change its state of motion when a force is applied [36]. According to this, large inertial masses accelerate more slowly than lighter ones and vice versa [6]. Heavy masses correspond to the better solutions.

Therefore, they should change their position very little (similar to *gbest* in PSO) and must attract the other solutions which depend on the other masses and distance between them and successively change their motions slowly.

Finally, the $(t+1)$th velocity of ith mass in the dimension d and its updated position can be calculated as (46) and (47), respectively.

$$v_i^d(t+1) = \text{rand}_{1i} \times v_i^d(t) + a_i^d(t) \tag{46}$$

$$x_i^d(t+1) = x_i^d(t) + v_i^d(t+1) \tag{47}$$

The updated mass i in time t may be expressed as follows

$$m_i(t) = \frac{\text{fit}_i(t) - \text{worst}(t)}{\text{best}(t) - \text{worst}(t)} \tag{48}$$

$$M_i(t) = \frac{m_i(t)}{\sum_{j=1}^{N} m_j(t)} \tag{49}$$

where

$$\text{best}(t) = \min_{j\in\{1,2,\ldots,N\}} \text{fit}_j(t) \tag{50}$$

$$\text{worst}(t) = \max_{j\in\{1,2,\ldots,N\}} \text{fit}_j(t) \tag{51}$$

and where $\text{fit}_i(t)$ represents the fitness value of the ith mass in time t. In the following section, the presented concepts are employed to form the proposed algorithm.

4.2. Proposed modifications applied to GSA

In this paper, following modifications are implemented to improve performance of GSA as follows.

4.2.1. Calculating gravitational constant based on standard gravitational parameter

In the real world, measuring the gravitational constant with high accuracy is difficult while determining standard gravitational parameter, denoted by μ, with acceptable precision is possible. Hence, the parameter $\mu(t)$ at iteration tth is calculated by the product of the gravitational constant and sum of two mass i and j as follows (general representation [40]):

$$\mu(t) = G_0 \times \left(M_i(t) + M_j(t)\right) \tag{52}$$

So, (41) can be modified as follows:

$$G_{ij}(t) = \frac{\mu(t)}{M_i(t) + M_j(t)} \times \exp\left(\frac{-\delta t}{\text{Iteration}_{\max}}\right) \tag{53}$$

The above equations shows a proper gravitational constant between two specific mass i and j. This is against (41) which assumed a gravitational constant for all masses.

In this paper, $\mu(t)$ will be reduced with time to control the search accuracy and provide better performance:

$$\mu(t) = \frac{\xi}{t} \tag{54}$$

where ξ is a constant term.

4.2.2. A new self-adaptive learning strategy for GSA

In this strategy, two updating methods are applied in a probabilistic manner to GSA in order to increase its performance. In fact, a more profitable method than other is selected to adaptively give preference to appropriate mutation at each iteration. In this regard, a probability value is assigned to each of the updating methods. This value is dependent on the ability of the corresponding updating method to provide more optimal solutions based on an appropriate adaptively updating mechanism. Two updating methods are as follows:

Technique 1: this method acts as G_{best}-guided in PSO and uses time varying acceleration coefficient as TVAC-PSO [41]. So, (47) is modified as follows:

$$x_i^d(t+1) = x_i^d(t) + v_i^d(t+1) + AC(t) \times \text{rand}_{2i} \times \left(G_{\text{best}} - x_i^d(t)\right), \;\; i = 1, \dots, NT_1 \tag{55}$$

where

$$AC(t) = AC_{\text{initial}} + \frac{AC_{\text{final}} - AC_{\text{initial}}}{\text{Iteration}_{\max}} \times t$$

and where AC is acceleration coefficient in which AC_{initial} and AC_{final} represent the relevant initial and final values; rand_{2i} is a random number in the interval $[0,1]$; NT_1 denotes the number of masses which update through Technique 1.

The third term of the right hand side of (47), exploits an exterior memory for obtaining the best solution called G_{best} which obtained from solutions saved until now. To improve the solution quality, $AC(t)$ should be increased at each iteration, i.e. $AC_{\text{final}} > AC_{\text{initial}}$. This is because of the fact that, at the beginning, the high value of $AC(t)$ leads masses to a local optimum prematurely.

Note that, by selecting this method, the effect of difference $\left(G_{\text{best}} - x_i^d(t)\right)$, by applying $AC(t) \times \text{rand}_{2i}$, is implemented which is different from other approaches suggested in literature such as [42,43].

Technique 2: it is adapted to improve the diversity of the solutions, avoid being trapped in local optima. In this method, five different masses are selected randomly for each mass i such that $i \neq i1 \neq i2 \neq i3 \neq i4 \neq i5$. So, a trail solution is calculated as follows [42,43]:

$$x_{i,\text{trail}}^d(t+1) = x_{i1}^d(t) + \text{rand}_{3i} \times \left(x_{i2}^d(t) - x_{i3}^d(t)\right) + \text{rand}_{4i} \times \left(x_{i4}^d(t) - x_{i5}^d(t)\right), \quad i = 1, \dots, NT_2 \tag{56}$$

where rand_{3i} and rand_{4i} are two random numbers in the interval $[0,1]$; NT_2 denotes the number of masses which update through Technique 2.

This technique can be identified as follows:

$$x_i^d(t+1) = \begin{cases} x_{i,\text{trail}}^d(t+1) & \text{if } \text{rand}_{5i} \leq 0.5 \\ x_i^d(t+1) & \text{else} \end{cases} \tag{57}$$

where rand_{5i} is a random number in the interval $[0,1]$.

The probability of both mentioned techniques are calculated as follows [44]:

$$\text{Prob}_{\text{Technique}_i} = (1-\theta) \times \text{Prob}_{\text{Technique}_i} + \frac{\theta \times AP_{\text{Technique}_i}}{\text{Iteration}_{\max}}, \;\; i = 1, 2 \tag{58}$$

where θ denotes the learning factor which is selected as $\theta = 0.142$ [42–44]; $AP_{\text{Technique}_i}$ is the accumulator for the ith presented technique and can be updated as:

$$AP_{\text{Technique}_i} = AP_{\text{Technique}_i} + wf_j, \qquad j = 1, \dots, NT_i \text{ and } i = 1, 2 \tag{59}$$

where wf represents a weight factor for each technique. This factor leads to better solution selection through applying larger weight and can be determined as follows:

$$wf_j = \frac{\log(N-j+1)}{\log(1)+\cdots,\log(N)}, \qquad j = 1,\ldots,N \tag{60}$$

Finally, the normalized probabilities related to each technique are calculated as follows:

$$\mathrm{Prob}_{\mathrm{Technique}_i} = \frac{\mathrm{Prob}_{\mathrm{Technique}_i}}{\sum_{i=1}^{2}\mathrm{Prob}_{\mathrm{Technique}_i}}, \ \ i = 1, 2 \tag{61}$$

In summary, this subsection presented two different updating technique based on a probabilistic way. The first technique uses G_{best} applying time varying acceleration coefficient. The second technique is utilized to diverse the solutions through selecting five different masses. In this method, if a random number is larger than 0.5, then conventional updating strategy (47) is selected; else, (57) is used. The selection method for each technique is illustrated in the following section.

4.3. Differences between SAL-TVAC-GSA and TVAC-GSA

The main differences between the proposed method and an improved version of GSA, i.e. TVAC-GSA, are summarized as follows:

- In TVAC-GSA only one movement strategy is applied to update positions while in SAL-TVAC-GSA three different updating procedures are adopted.
- In SAL-TVAC-GSA, G_0 is calculated based on two involved masses while in TVAC-GSA it is selected at the beginning (in the first step). In other words, in TVAC-GSA, this parameter is constant over all iterations while in SAL-TVAC-GSA it is updated at each iteration (a self-adaptive parameter).
- In SAL-TVAC-GSA, the best movement strategy is used in a probabilistic manner. In fact, a more profitable movement dependent on the ability of the corresponding updating approach to provide a better quality solution is selected.
- In SAL-TVAC-GSA, there is an updating method to diverse the solutions, avoid being trapped in local optimum. This method reflects a totally random movement pattern.

5. SAL-TAVC-GSA for EHED problem

Solving EHED problem in the form of minimizing (31) or (32) or (33) subject to (34)–(38), will be applied through different steps illustrated in Fig. 6. These steps are expressed as:

Step 1. Initialize the parameters of SAL-TVAC-GSA, i.e. N, K_0, ξ, δ, AC_{initial}, AC_{final}, $\mathrm{Iteration}_{\mathrm{max}}$, and initial values of Prob and AP.

Step 2. Set initial control variables as initial positions of all masses within their limits. In the EHED problem, the energy production of all sources and all dispatch factors are independent variables which can be randomly selected within their limits.

Step 3. Calculate the value of fitness for all masses. In this work, the penalty method to meet all equality constraints has been selected as below:

$$\mathrm{fit} = OF_k + W_1\left(\sum_{i=1}^{N_{hub}} \mathbf{C}_i\mathbf{Output}_i - \mathbf{Input}_i\right)^2 + W_2\left(\left(E_i^{\mathrm{demand}} - \sum_{j=1}^{N_{hub}} E_{j,i}^{\mathrm{out}}\right)_{i\in\{e,h,c,a\}}\right)^2, k = 1,2,3 \tag{48}$$

where W_1 and W_2 are two weighting factors (penalty parameters). It should be noted that, in order to achieve a feasible solution, the weighting factors of the penalty function are increased along the iterative process linearly.

Step 4. Update $G_{ij}(t)$, $\text{best}(t)$, $\text{worst}(t)$, and $M_i(t)$ for each set of masses. Also, calculate the total gravitational force using (44) for all agents. Then, determine their acceleration through (45).

Step 5. Calculate velocities using (46).

Step 6. Based on the Roulette Wheel Mechanism (RWM), one of the presented techniques for updating the position of each mass should be selected as follows: if $\text{Prob}_{\text{Technique}_i}$ becomes greater than a random number in interval [0, 1], then select *Technique 1*; otherwise, select *Technique 2*.

Step 7. Check that all control variables are within their limits. If any of them violates or hits the limit, set it at its limit value (upper or lower).

Step 8. If the age of algorithm (i.e. iteration) is equal or less than the maximum iteration (i.e. $t \leq \text{Iteration}_{\text{max}}$), then repeat Step 3–7. Otherwise, go to Step 9.

Step 9. Print the best results.

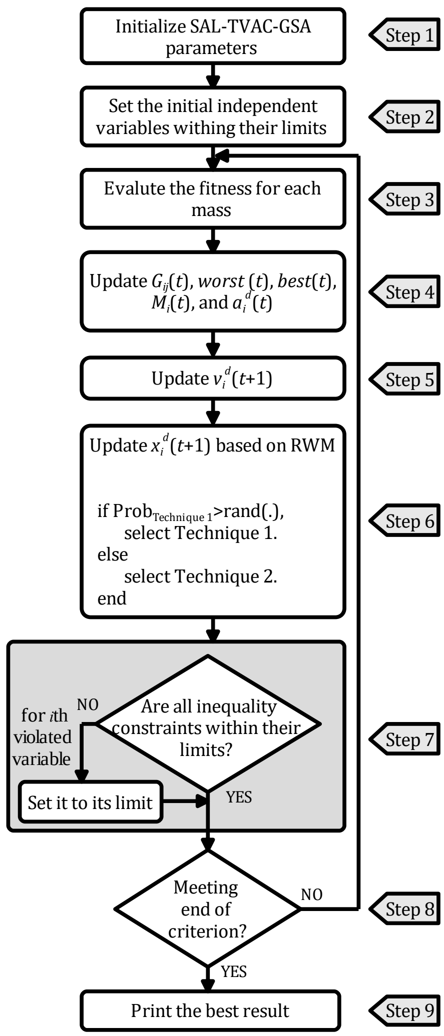

Fig. 6. Flowchart of the proposed SAL-TVAC-GSA-based EHED.

6. Simulation results

The proposed SAL-TVAC-GSA-based EHED is tested on a new highly nonlinear, non-convex, non-smooth, non-differential and high-dimensional system with 103 control variables (76 variables for sources and the rest for dispatch factors). Simulation is carried out on this network including 76 sources consist of 27 electrical sources with valve-point loading effect (some of them with prohibited operating zones), 34 gas stations, and 15 heat sources to supply 39 hubs with 29 structures presented in subsection 2.2. The total demand of the networks associated with electricity (i.e. E_e^{demand}), heating (i.e. E_h^{demand}), cooling (i.e. E_c^{demand}), and compressed air (i.e. E_a^{demand}) are 12.0, 9.5, 0.7, and 1.2 pu, respectively. The system data is given in Appendix A. Before go further, it should be mentioned that to test the SAL-TVAC-GSA performance, it is evaluated on a set of five benchmark functions and the obtained results are presented in Appendix B.

The suggested method is programmed in MATLAB environment and implemented on an Intel Pentium CPU, 2.0 GHz with 2GB RAM, PC. In order to attain the best quality solution with a good convergence speed, the optimum setting of various SAL-TVAC-GSA parameters should be selected. Hence, different trails for a specific system should be performed to meet the best setting. Accordingly different parameters of SAL-TVAC-GSA are defined as: $\xi = 0.001$, $\delta = 1$, $N = K_0 = 50$, $AC_{\text{initial}} = 0.5$, $AC_{\text{final}} = 1.5$, $\text{Iteration}_{\max} = 200$, $\text{Prob}_{\text{Technique}_1} = 0.5$, $\text{Prob}_{\text{Technique}_2} = 0.5$, $AP_{\text{Technique}_1} = 0$, and $AP_{\text{Technique}_2} = 0$.

In this section, the best results in terms of quality solution and convergence speed over 30 independent runs are compared with various programmed algorithms such as GA, PSO, GSA, TVAC-GSA, and EGSA (see [42,43]) to illustrate the ability of the proposed algorithm in finding an operating point with lower objective function. Also, all results are in a per-unit (pu) system and all costs are in monetary-unit (mu). It should be noted that, all methods ensure that all constraints are satisfied.

6.1. Case 1: Minimization of energy cost as a single-objective problem

The obtained optimal solution by the introduced method through minimizing (31) subject to (34)–(38) (or optimizing (48) with $k = 1$ subject to (36)–(38)) is compared with those that found by TVAC-GSA, EGSA, GSA, PSO and GA in Table 1. This table shows that the optimal operating point searched by the proposed technique in terms of quality solution, objective function, and computational time is better than those obtained by all other analyzed approaches. The objective value reached by SAL-TVAC-GSA is 15,728.3913 mu, whereas the optimal values of the objective function searched by TVAC-GSA, EGSA, GSA, PSO, and GA approaches are 15,747.3098, 15,751.6029, 15,870.0549, 16,106.0947, and 16,384.4316 mu, respectively. This improvement results in more annual cost saving assuming constant load level. Fig. 7 reflects this result and indicates that a little cost improvement can save the annual cost significantly.

Based on Table 1, the total energy production obtained by GA, PSO, GSA, EGSA, TVAC-GSA, and the suggested method is 27.4788, 27.1058, 27.9239, 27.0377, 27.0459, and 27.0706 pu, respectively. Also, the total energy losses in hubs obtained by the mentioned techniques are 4.0788, 3.7058, 4.5232, 3.6376, 3.6459, and 3.6706 pu, respectively. Moreover, the proposed method with about 17.2 seconds is faster than all other techniques. This shows about 9% time saving (average). Fig. 8 illustrates dispatch factors related to the input and output of all hubs obtained by SAL-TVAC-GSA. It can be easily seen that these variables are in their acceptable ranges. Finally, Fig. 9 represents the convergence characteristic curves of all analyzed algorithms.

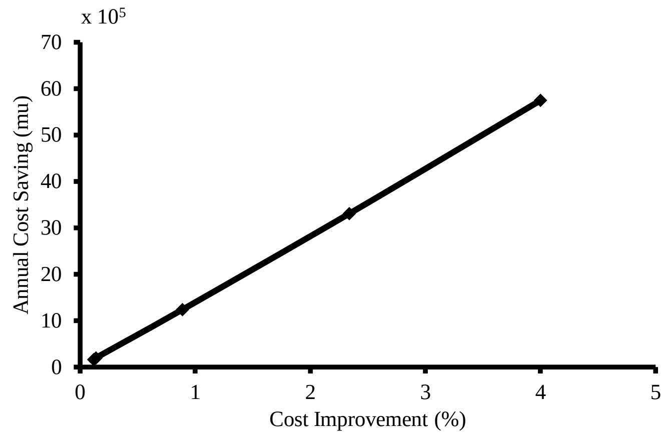

Fig. 7. Impact of cost improvement on the annual cost saving

Table 1. Comparative results using different techniques-energy cost minimization

Hub Code	Hub Type	Energy Type	Optimal Production (pu)					
			GA	PSO	GSA	EGSA	TVAC-GSA	SAL-TVAC-GSA
A1	#1	Electricity	0.1000	0.1000	0.1000	0.1020	0.1000	0.1003
A2	#1	Electricity	0.4000	0.4000	0.4037	0.4072	0.4003	0.4041
B1	#2	Gas	0.5000	0.5000	0.5000	0.5014	0.5003	0.5001
C1	#3	Gas	1.8984	0.3044	0.3417	0.3515	0.3227	0.3522
D1	#4	Gas	0.1345	0.9610	0.5993	0.5742	0.6367	0.5865
E1	#5	Heat	0.3636	0.2000	0.2000	0.2000	0.2013	0.2007
F1	#6	Electricity	0.2000	0.2000	0.2000	0.2000	0.2001	0.2000
		Gas	0.1000	0.4255	0.1079	0.1068	0.1040	0.1074
F2	#6	Electricity	0.3000	0.3000	0.3007	0.3042	0.3027	0.3036
		Gas	1.3382	0.9565	1.0583	1.1857	1.0078	1.1092
G1	#7	Electricity	0.8493	0.1000	0.8663	0.8663	0.8693	0.8744
H1	#8	Electricity	0.2000	1.5000	0.2391	0.2280	0.2127	0.2304
		Gas	0.3655	0.3285	0.2000	0.2007	0.2009	0.2002
I1	#9	Gas	0.1500	0.1500	0.1739	0.1721	0.1762	0.1721
J1	#10	Gas	0.1000	0.1000	0.1944	0.1867	0.1959	0.2236
		Heat	0.2000	0.2014	0.2000	0.2062	0.2030	0.2039
K1	#11	Gas	0.1000	0.1000	0.1239	0.1178	0.1189	0.1303
		Heat	0.2001	0.2000	0.2000	0.2001	0.2007	0.2000
L1	#12	Gas	0.3000	0.3000	0.3001	0.3001	0.3003	0.3000
M1	#13	Electricity	0.1010	0.1000	0.1096	0.1239	0.1106	0.1169
		Heat	0.1000	0.1000	0.4888	0.4950	0.4683	0.4646
N1	#14	Electricity	0.1000	0.1000	0.1021	0.1030	0.1005	0.1002
		Gas	1.1255	0.2000	1.5872	1.5831	1.6168	1.5558
O1	#15	Gas	0.3308	0.4976	0.5486	0.5300	0.5230	0.5023
		Heat	0.1000	0.1000	0.1000	0.1021	0.1003	0.1002
P1	#16	Gas	0.1000	0.1064	0.3465	0.3121	0.3438	0.3315
Q1	#17	Gas	0.1000	0.2240	0.4303	0.4546	0.4830	0.4109
Q2	#17	Gas	0.7447	0.2000	0.2091	0.2105	0.2086	0.2139
R1	#18	Electricity	0.3000	1.5911	1.6375	1.6053	1.6101	1.6092
		Gas	0.1243	0.1000	0.1000	0.1001	0.1010	0.1001
		Heat	0.1879	0.1000	0.2154	0.1887	0.2086	0.2074
S1	#19	Electricity	0.2000	0.2000	0.2000	0.2046	0.2001	0.2010
		Gas	0.2000	0.2000	0.2012	0.2004	0.2031	0.2007
		Heat	0.3137	0.7000	0.1977	0.2138	0.1999	0.1895
S2	#19	Electricity	2.1000	0.1000	0.8861	0.8939	0.8934	0.8859
		Gas	0.1000	0.1000	0.1141	0.1177	0.1058	0.1108
		Heat	0.9000	0.1000	0.1112	0.1113	0.1121	0.1172
S3	#19	Electricity	0.1000	0.1000	0.1000	0.1009	0.1000	0.1000
		Gas	0.1000	0.1000	0.1997	0.1970	0.2450	0.2190
		Heat	0.1000	0.1000	0.1000	0.1015	0.1001	0.1005

T1	#20	Electricity	0.7133	0.1000	0.1230	0.1192	0.1220	0.1175
		Gas	0.5701	0.3000	0.3000	0.3080	0.3007	0.3013
T2	#20	Electricity	0.2107	0.1000	0.1000	0.1000	0.1002	0.1003
		Gas	0.3737	0.3000	0.3059	0.3066	0.3076	0.3065
U1	#21	Electricity	0.1000	0.1000	0.8999	0.9116	0.8834	0.9017
		Gas	0.3000	0.3000	0.3000	0.3013	0.3000	0.3000
V1	#22	Electricity	0.2000	0.2000	0.2000	0.2022	0.2005	0.2000
		Gas	0.1000	1.3834	0.9573	0.9861	0.9623	0.9591
W1	#23	Electricity	0.1000	0.1000	0.1082	0.1050	0.1095	0.1050
		Gas	1.9000	1.9000	0.9181	0.8540	0.9353	0.9435
W2	#23	Electricity	0.3000	0.3000	0.3000	0.3000	0.3026	0.3008
		Gas	0.1000	1.4000	0.9821	0.9523	0.9859	0.9834
X1	#24	Electricity	0.2000	0.9115	0.2000	0.2001	0.2003	0.2015
		Gas	0.2000	0.3930	0.2035	0.2002	0.2015	0.2049
Y1	#25	Electricity	2.5839	3.0000	2.7226	2.7053	2.7542	2.7001
		Gas	0.1000	0.1000	0.9821	0.1000	0.1001	0.1001
Y2	#25	Electricity	0.5004	0.0000	0.0153	0.0175	0.0111	0.0137
		Gas	0.1000	0.1454	0.1191	0.1159	0.1214	0.1238
Z1	#26	Electricity	0.1000	0.1000	0.1000	0.1004	0.1015	0.1016
		Gas	0.1000	0.1936	0.1128	0.1182	0.1238	0.1187
		Heat	0.1097	0.1000	0.4355	0.4475	0.4522	0.4735
Γ1	#27	Electricity	0.2001	0.2000	0.2000	0.2000	0.2010	0.2051
		Gas	0.2000	0.2000	0.2000	0.2001	0.2000	0.2001
		Heat	0.1000	0.3338	0.1045	0.1004	0.1001	0.1023
Γ2	#27	Electricity	0.1000	0.1000	0.1000	0.1000	0.1001	0.1002
		Gas	0.2074	0.2000	0.2834	0.2864	0.2355	0.3007
		Heat	0.2540	0.2000	0.2003	0.2003	0.2007	0.2021
Ψ1	#28	Electricity	0.9000	0.9000	0.8268	0.8303	0.8268	0.8269
		Gas	0.1000	0.1000	0.1407	0.1460	0.1428	0.1324
		Heat	0.2000	0.2000	0.2000	0.2015	0.2003	0.2003
Σ1	#29	Electricity	0.1000	0.1000	0.1354	0.1359	0.1350	0.1313
		Gas	0.1000	0.1000	0.1481	0.1400	0.1438	0.1455
		Heat	0.1004	0.1000	0.2138	0.2083	0.2124	0.2095
Σ2	#29	Electricity	0.2000	0.2000	0.2000	0.2018	0.2001	0.2000
		Gas	0.3276	0.1000	0.1859	0.1722	0.1764	0.2150
		Heat	0.1000	0.1987	0.1045	0.1029	0.1067	0.1061
Total Production (pu)		Electricity	11.4587	11.2026	11.3763	11.3686	11.3481	11.3315
		Gas	12.6907	12.9693	13.4752	12.5897	12.6313	12.6614
		Heat	3.3294	2.9339	3.0717	3.0794	3.0665	3.0777
Total Losses (pu)			4.0788	3.7058	4.5232	3.6376	3.6459	3.6706
Cost (mu)			16384.4316	16106.0947	15870.0549	15751.6029	15747.3098	15728.3913
Objective Function (mu)			16384.4316	16106.0947	15870.0549	15751.6029	15747.3098	15728.3913
Computational Time (s)			27.3846	18.5038	17.3926	17.2627	17.3030	17.2354

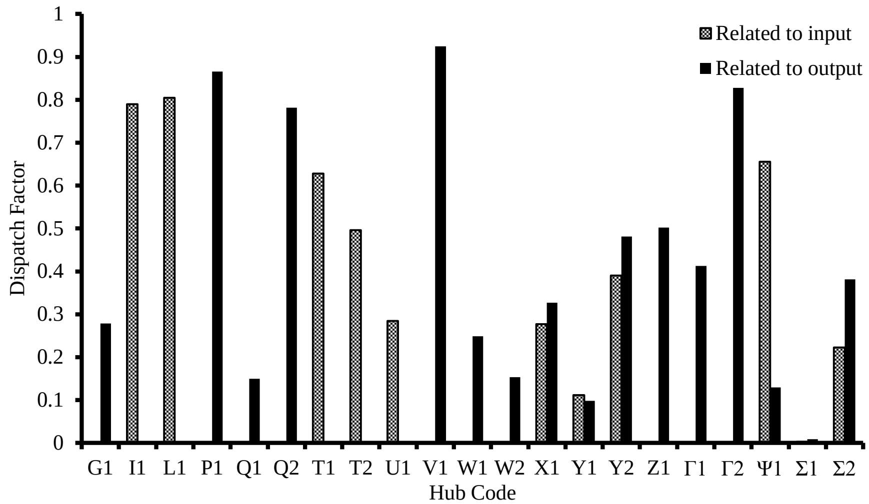

Fig. 8. Dispatch factors of all hubs obtained by SAL-TVAC-GSA for energy cost minimization

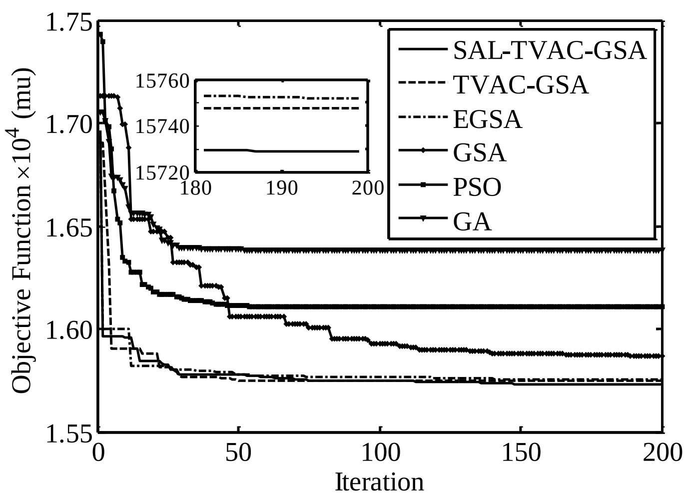

Fig. 9. Convergence characteristics for energy cost minimization

In the analyzed system, hub code T1 with hub type #20 is selected to show how energy is consumed, converted, and finally delivered to the loads. This hub is depicted in Fig. 10. According to the obtained results of SAL-TVAC-GSA, this hub consumes 0.1175 and 0.3013 pu electricity and gas, respectively. These values are 1.03 and 2.37% of total electricity and gas generations, respectively. Based on optimal dispatch factor $\nu = 62.819\%$, 0.1893 pu of the entire gas is used by CHP unit and the rest is consumed by gas furnace. The entire electricity is completely delivered to transformer. After energy conversion by the mentioned elements, two types of energy, i.e. electricity and heat, are available at the output. CHP generates 0.0663 pu electrical power which is added to 0.1175 pu to supply 1.53% of total electrical demand. Moreover, the produced heat by gas furnace (0.0728 pu) and CHP (0.0852 pu) supplies 1.66% of total heat demand. Meanwhile, the hub loss is 0.0770 pu (2.09% of total energy losses) and the energy cost of this hub is 171.3114 mu (1.09% of total energy cost).

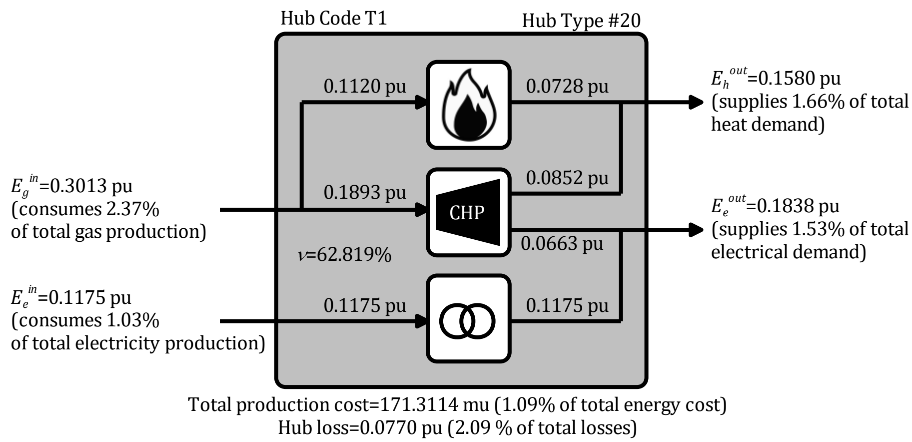

Fig. 10. Energy conversion of hub code T1 (hub type #20) based on results of SAL-TVAC-GSA in Case 1

6.2. Case 2: Minimization of energy losses as a single-objective problem

The aim of this subsection is to minimize (32) subject to (34)–(38) (or optimize (48) with $k = 2$ subject to (36)–(38)). The obtained results by SAL-TVAC-GSA in terms of optimal energy production (along with total electricity, gas, and heat generations), total losses (as the objective function), energy cost, as well as computational time are compared with those found by TVAC-GSA, EGSA, GSA, PSO, and GA in Table 2. Moreover, Fig. 11 reflects dispatch factors of all hubs related to SAL-TVAC-GSA solution. It can be seen that, the proposed algorithm can reach to a better quality solution with lower losses and CPU time. The energy cost searched by SAL-TVAC-GSA, TVAC-GSA, EGSA, GSA, PSO, and GA are about 16825, 16811, 16824, 17308, 16858, and 16623 mu, respectively. In this viewpoint, the proposed approach results in about 1.2% increasing in the energy cost. It is because of the fact that in this case, the energy cost is not important (it is not included in the objective function). Moreover, the energy losses found by the mentioned techniques are 2.8100, 2.8317, 2.8162, 2.9385, 2.9950, and 3.3902 pu, respectively. Average computational time improvement is about 16.9 seconds. Also, total energy productions obtained by the mentioned algorithms are 26.2100, 26.2369, 26.2162, 26.3385, 26.3950, and 26.7902 pu, respectively. It is clear that based on (32) this type of problem should search a lower energy production level. Convergence characteristic curves of all tested algorithms are shown in Fig. 12.

Table 2. Comparative results using different techniques-energy loss minimization

Hub Code	Hub Type	Energy Type	Optimal Production (pu)					
			GA	PSO	GSA	EGSA	TVAC-GSA	SAL-TVAC-GSA
A1	#1	Electricity	0.1679	0.1031	0.7438	0.7469	0.7500	0.7498
A2	#1	Electricity	0.4818	0.4000	0.4000	0.4000	0.4000	0.4002
B1	#2	Gas	0.5075	0.5000	0.5026	0.5000	0.5006	0.5000
C1	#3	Gas	0.3521	0.8796	0.3656	0.3000	0.3000	0.3000
D1	#4	Gas	0.1622	0.1000	0.1295	0.1000	0.1001	0.1000
E1	#5	Heat	0.2405	0.2167	0.2044	0.5000	0.5000	0.4999
F1	#6	Electricity	0.2408	0.9331	0.2000	1.2500	1.2500	1.2500
		Gas	0.1125	0.1144	0.1111	0.1000	0.1000	0.1000
F2	#6	Electricity	0.3539	1.7404	1.7500	0.3007	0.3006	0.3000
		Gas	0.2384	0.1000	0.4655	1.4000	1.4000	1.4000
G1	#7	Electricity	0.8798	0.9991	0.1039	0.1080	0.1040	0.1087
H1	#8	Electricity	1.1270	0.2006	0.5254	0.2000	0.2000	0.2000
		Gas	0.2229	0.2000	0.2058	0.2240	0.2336	0.2231
I1	#9	Gas	0.3219	0.1947	0.2693	0.1500	0.1500	0.1502
J1	#10	Gas	0.3349	1.0234	0.3984	0.1958	0.2703	0.1936
		Heat	0.2086	0.3184	0.4702	0.4996	0.4995	0.4991

K1	#11	Gas	0.3239	0.1000	0.3549	0.1001	0.1000	0.1000
		Heat	0.2074	0.5000	0.2747	0.2000	0.2000	0.2000
L1	#12	Gas	0.3679	1.1099	0.8512	0.3000	0.3001	0.3000
M1	#13	Electricity	0.2369	0.7270	0.7500	0.2766	0.2761	0.2778
		Heat	0.6043	0.7630	0.3299	0.1000	0.1001	0.1001
N1	#14	Electricity	0.1001	0.7500	0.1073	0.1593	0.1513	0.1562
		Gas	1.8186	0.3733	0.2094	0.2000	0.2004	0.2000
O1	#15	Gas	0.3066	0.1000	0.1117	0.1000	0.1000	0.1000
		Heat	0.1615	0.3216	0.1076	0.1000	0.1000	0.1000
P1	#16	Gas	0.3291	0.1000	0.5329	0.1321	0.1358	0.1311
Q1	#17	Gas	0.1422	0.1000	0.1027	0.1000	0.1000	0.1000
Q2	#17	Gas	0.2268	0.2022	0.2000	0.2000	0.2000	0.2000
R1	#18	Electricity	0.9549	0.9981	0.3995	1.7500	1.7497	1.7500
		Gas	0.1905	0.1000	0.1000	1.0965	1.0879	1.0981
		Heat	0.3347	0.2465	0.8812	0.9000	0.8996	0.9000
S1	#19	Electricity	0.7789	0.2080	0.7807	1.0988	1.1000	1.0995
		Gas	0.2432	0.2000	0.2521	0.2001	0.2002	0.2000
		Heat	0.2749	0.7000	0.6309	0.4517	0.4525	0.4611
S2	#19	Electricity	0.8853	0.8884	0.1374	0.1002	0.1000	0.1000
		Gas	0.2036	0.1000	0.1019	0.1000	0.1000	0.1000
		Heat	0.1386	0.1000	0.1003	0.1000	0.1001	0.1000
S3	#19	Electricity	0.1086	0.1385	0.1712	0.1000	0.1000	0.1000
		Gas	0.1274	0.1000	0.1000	0.1000	0.1000	0.1000
		Heat	0.1053	0.2451	0.1256	0.1000	0.1000	0.1000
T1	#20	Electricity	0.1259	0.1000	0.7500	0.7500	0.7499	0.7499
		Gas	0.3594	0.3030	0.3520	0.3000	0.3003	0.3000
T2	#20	Electricity	0.1577	0.1016	0.2794	0.1000	0.1000	0.1000
		Gas	0.3789	0.3000	0.3156	0.3351	0.3178	0.3325
U1	#21	Electricity	1.4026	0.3015	1.1662	0.1000	0.1000	0.1002
		Gas	0.3002	0.3000	0.3053	0.3005	0.3001	0.3000
V1	#22	Electricity	0.2024	0.2862	0.2729	0.2367	0.2174	0.2431
		Gas	0.4828	0.1000	0.1261	0.1001	0.1000	0.1000
W1	#23	Electricity	0.1112	0.1309	0.1000	0.7500	0.7500	0.7500
		Gas	0.6799	0.2085	0.2184	0.2143	0.2095	0.2032
W2	#23	Electricity	0.3016	0.7974	0.3000	0.3002	0.3000	0.3000
		Gas	0.9461	0.1907	0.7903	1.4000	1.4000	1.4000
X1	#24	Electricity	0.2000	0.2378	0.2000	0.2000	0.2000	0.2000
		Gas	0.2634	0.2000	0.2096	0.2000	0.2000	0.2000
Y1	#25	Electricity	0.9540	0.0027	0.0000	0.0000	0.0000	0.0000
		Gas	0.1022	0.1000	0.1007	0.1000	0.1000	0.1000
Y2	#25	Electricity	0.0688	0.2005	0.2919	0.0000	0.0000	0.0000
		Gas	0.1327	0.1000	0.4514	0.1000	0.1002	0.1001
Z1	#26	Electricity	0.1572	0.1000	0.2022	0.1000	0.1000	0.1000
		Gas	0.1000	0.7308	0.1179	0.1001	0.1000	0.1000
		Heat	0.2515	0.1194	0.1000	0.1000	0.1000	0.1000
Γ1	#27	Electricity	0.2727	0.2149	0.9071	0.2000	0.2000	0.2000
		Gas	0.2526	0.7463	0.2068	0.2000	0.2000	0.2000
		Heat	0.1147	0.1000	0.5000	0.5000	0.4997	0.5000
Γ2	#27	Electricity	0.1034	0.1000	0.1000	1.1000	1.1000	1.1000
		Gas	0.4075	0.2000	0.3258	0.2000	0.2002	0.2000
		Heat	0.2049	0.2000	0.2015	0.2000	0.2000	0.2000
Ψ1	#28	Electricity	0.9000	0.8976	0.0565	0.9000	0.9000	0.8995
		Gas	0.1387	0.1000	0.1000	0.1000	0.1000	0.1000
		Heat	0.2078	0.2050	0.2000	0.2000	0.2000	0.2000
Σ1	#29	Electricity	0.2239	0.1000	0.1427	0.1000	0.1000	0.1000
		Gas	0.2067	0.3161	0.4159	0.1000	0.1000	0.1000
		Heat	0.2051	0.1161	0.3412	0.1409	0.1263	0.1374
Σ2	#29	Electricity	0.2018	0.2000	1.0805	0.5479	0.5512	0.5454
		Gas	0.1252	0.1183	0.1811	0.1000	0.1000	0.1000
		Heat	0.4228	0.6746	0.3709	0.8000	0.8000	0.8000
Total Production (pu)		Electricity	11.6991	11.8574	11.9186	11.8753	11.8555	11.8803
		Gas	11.4085	9.7112	9.5815	9.4488	9.5035	9.4320
		Heat	3.6826	4.8264	4.8384	4.8922	4.8779	4.8977

Total Losses (pu)	3.3902	2.9950	2.9385	2.8162	2.8317	2.8100
Cost (mu)	16622.8797	16858.0050	17308.0887	16823.5307	16811.3114	16824.7134
Objective Function (pu)	3.3902	2.9950	2.9385	2.8162	2.8317	2.8100
Computational Time (s)	17.2353	11.7354	9.9919	9.6391	9.5825	9.2078

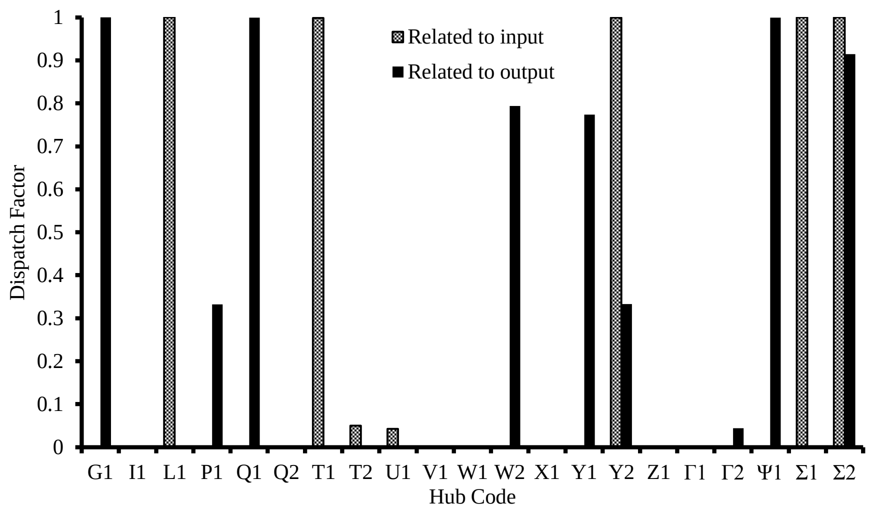

Fig. 11 . Dispatch factors of all hubs obtained by SAL-TVAC-GSA for energy loss minimization

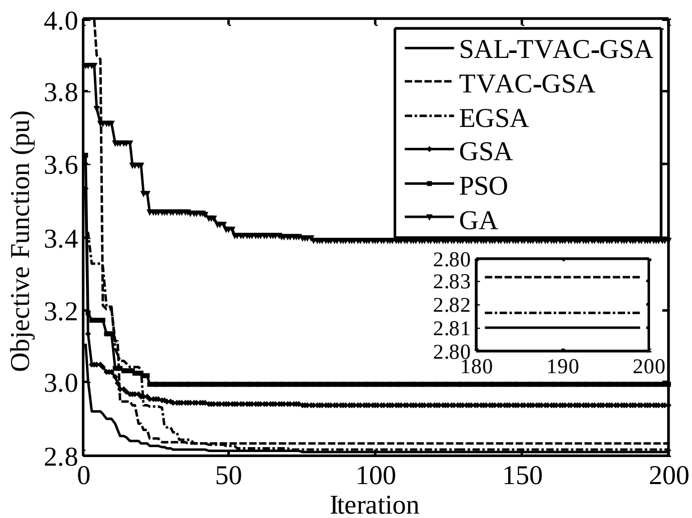

Fig. 12. Convergence characteristics for energy loss minimization

6.3. *Case 3: Minimization of energy cost and losses simultaneously as a multi-objective problem*

In order to demonstrate the effectiveness of the proposed SAL-TVAC-GSA to solve multi-objective problems, energy cost and hub losses are optimized simultaneously. For this purpose, minimizing (33) subject to (34)–(38) (or optimizing (48) with $k = 3$ subject to (36)–(38)) is investigated. The optimal values of energy production and objective function related to the suggested technique and TVAC-GSA, EGSA, GSA, PSO, and GA are tabulated in Table 3. Moreover, total production of each carrier, total energy cost and losses, as well as computational time of the mentioned algorithms are illustrated in this table. It can be observed that when energy cost along with energy loss is simultaneously minimized, the objective function value obtained by the proposed algorithm is about 18169 mu, whereas the optimal values of objective function searched by TVAC-GSA, EGSA, GSA, PSO, and GA approaches are about 18199, 18188, 18273, 18588, and 18960 mu, respectively. Moreover, the suggested approach provides a lower energy cost and computational time if compared with all other presented algorithms. In fact, the obtained energy costs by the mentioned algorithms are about 15730, 15752, 15755, 15965, 16402, and 16389 mu, respectively. Also, the average computational time is about 20.7 seconds while for the GSA family (i.e. GSA, EGSA, TVAC-GSA, and SAL-TVAC-GSA) it is about 18.7 seconds. Theses mean that employing different versions of GSA leads to the better results in terms of both quality solution and computational time. Moreover, these clearly indicate that SAL-TVAC-GSA outperforms the other presented techniques. The average annual cost saving assuming constant load level is about 2820855 mu for about 2% cost improvement. This indicates that a little cost improvement can significantly save the cost. Consequently, discrimination for real-life applications should be done on the basis of searching the better results, i.e. the capability to provide a better quality solution considering economical benefits without convergence problems. The optimal values of dispatch factors of all hubs related to SAL-TVAC-GSA solution are illustrated in Fig. 13. Furthermore, convergence curves of all analyzed algorithms are depicted in Fig. 14.

Table 3. Comparative results using different techniques-minimization of energy cost and losses

Hub Code	Hub Type	Energy Type	Optimal Production (pu)					
			GA	PSO	GSA	EGSA	TVAC-GSA	SAL-TVAC-GSA
A1	#1	Electricity	0.1244	0.1000	0.1014	0.1000	0.1000	0.1005
A2	#1	Electricity	0.4153	0.4000	0.4000	0.4038	0.4035	0.4000
B1	#2	Gas	0.5474	0.5000	0.5013	0.5002	0.5000	0.5069
C1	#3	Gas	0.3291	0.4001	0.4368	0.3266	0.3421	0.3428
D1	#4	Gas	0.3409	0.1000	0.5094	0.6481	0.6036	0.5939
E1	#5	Heat	0.2000	0.2141	0.2112	0.2010	0.2002	0.2000
F1	#6	Electricity	0.2835	0.2103	0.2006	0.2000	0.2004	0.2020
		Gas	0.1465	0.8476	0.1000	0.1000	0.1082	0.1160
F2	#6	Electricity	0.3011	0.3001	0.3062	0.3067	0.3003	0.3000
		Gas	0.7551	0.1000	0.9249	1.0361	1.0619	1.0597
G1	#7	Electricity	0.8985	1.0000	0.9158	0.8754	0.8663	0.8639
H1	#8	Electricity	0.8241	0.3302	0.2689	0.2294	0.2387	0.2437
		Gas	0.3768	0.2795	0.2467	0.2000	0.2000	0.2000
I1	#9	Gas	0.1603	0.4000	0.2326	0.1728	0.1740	0.1759
J1	#10	Gas	0.1975	1.0955	0.1861	0.1864	0.1947	0.2028
		Heat	0.2420	0.4942	0.2000	0.2000	0.2000	0.2000
K1	#11	Gas	0.2616	0.1992	0.1002	0.1241	0.1241	0.1256
		Heat	0.3244	0.2573	0.2000	0.2044	0.2000	0.2025
L1	#12	Gas	0.4642	0.3306	0.3574	0.3076	0.3008	0.3017
M1	#13	Electricity	0.1281	0.1000	0.1375	0.1105	0.1094	0.1134
		Heat	0.2775	0.2843	0.6157	0.5015	0.4842	0.5010
N1	#14	Electricity	0.1161	0.7461	0.1016	0.1014	0.1018	0.1007
		Gas	1.6102	0.2000	1.8983	1.5933	1.5857	1.5754
O1	#15	Gas	0.1895	0.1247	0.1192	0.5379	0.5502	0.5193
		Heat	0.1629	0.1000	0.1181	0.1000	0.1000	0.1001
P1	#16	Gas	0.3313	0.1082	0.1584	0.3584	0.3447	0.3567
Q1	#17	Gas	0.2369	0.1000	0.1132	0.4241	0.4272	0.4599
Q2	#17	Gas	0.2031	0.3594	0.2293	0.2088	0.2088	0.2063
R1	#18	Electricity	0.9708	0.3017	1.5679	1.6297	1.6330	1.6095
		Gas	0.1044	0.1530	0.1028	0.1022	0.1000	0.1001
		Heat	0.1296	0.1983	0.1887	0.2205	0.2220	0.2167
S1	#19	Electricity	0.3742	1.1000	0.2000	0.2009	0.2000	0.2000
		Gas	0.2033	0.3708	0.2012	0.2015	0.2016	0.2052
		Heat	0.1629	0.5709	0.1297	0.2047	0.2008	0.2103
S2	#19	Electricity	1.6643	0.1005	1.6880	0.8912	0.8868	0.8854
		Gas	0.1087	0.1088	0.1211	0.1142	0.1128	0.1116

		Heat	0.1207	0.9000	0.1186	0.1136	0.1005	0.1178
S3	#19	Electricity	0.1023	0.1072	0.1034	0.1000	0.1000	0.1000
		Gas	0.1525	0.1509	0.2581	0.2201	0.1989	0.2431
		Heat	0.1431	0.1331	0.1411	0.1001	0.1000	0.1034
T1	#20	Electricity	0.1566	0.1574	0.1439	0.1217	0.1219	0.1249
		Gas	0.3528	0.4338	0.3433	0.3001	0.3002	0.3001
T2	#20	Electricity	0.1892	0.1000	0.1082	0.1019	0.1001	0.1001
		Gas	0.5529	0.3000	0.3274	0.3071	0.3057	0.3095
U1	#21	Electricity	0.1914	0.1026	0.9612	0.9232	0.9027	0.9056
		Gas	0.3819	0.3001	0.3000	0.3013	0.3004	0.3000
V1	#22	Electricity	0.2033	0.3709	0.2065	0.2000	0.2001	0.2003
		Gas	0.7376	0.1000	1.0649	0.9448	0.9575	0.9482
W1	#23	Electricity	0.1409	0.1007	0.1066	0.1128	0.1103	0.1000
		Gas	0.7607	0.6472	0.5136	0.9012	0.9099	0.9148
W2	#23	Electricity	0.3162	1.6813	0.3000	0.3001	0.3000	0.3000
		Gas	1.1029	0.1032	1.3347	0.9721	0.9755	0.9619
X1	#24	Electricity	0.2627	0.2000	0.2054	0.2003	0.2001	0.2010
		Gas	0.3442	0.6816	0.2549	0.2051	0.2040	0.2008
Y1	#25	Electricity	1.8365	2.8261	1.8909	2.7042	2.7292	2.6978
		Gas	0.1222	0.3547	0.1269	0.1002	0.1002	0.1001
Y2	#25	Electricity	0.3167	0.0073	0.0020	0.0171	0.0154	0.0127
		Gas	0.2425	0.1000	0.2459	0.1179	0.1189	0.1208
Z1	#26	Electricity	0.1000	0.1000	0.1047	0.1000	0.1000	0.1000
		Gas	0.2979	0.1000	0.1238	0.1087	0.1129	0.1112
		Heat	0.2016	0.1674	0.2044	0.4289	0.4334	0.4009
Γ1	#27	Electricity	0.2008	0.2000	0.2103	0.2006	0.2000	0.2003
		Gas	0.2061	0.2290	0.2168	0.2000	0.2002	0.2000
		Heat	0.1511	0.1370	0.1108	0.1001	0.1043	0.1097
Γ2	#27	Electricity	0.1103	0.1015	0.1000	0.1009	0.1000	0.1009
		Gas	0.2507	0.2000	0.2261	0.2754	0.2833	0.2228
		Heat	0.2965	0.2269	0.2311	0.2000	0.2001	0.2000
Ψ1	#28	Electricity	0.8146	0.0117	0.8292	0.8269	0.8267	0.8268
		Gas	0.1544	0.4013	0.1552	0.1417	0.1414	0.1434
		Heat	0.2000	0.2073	0.2084	0.2000	0.2000	0.2000
Σ1	#29	Electricity	0.2441	0.5676	0.1708	0.1356	0.1362	0.1635
		Gas	0.2358	0.6163	0.1401	0.1051	0.1478	0.1452
		Heat	0.2224	0.3984	0.1533	0.2203	0.2117	0.2130
Σ2	#29	Electricity	0.2036	0.2110	0.2201	0.2000	0.2000	0.2026
		Gas	0.1860	0.1000	0.1046	0.1779	0.1839	0.2156
		Heat	0.1000	0.1001	0.1269	0.1050	0.1049	0.1001
Total Production (pu)		Electricity	11.4896	11.5342	11.5511	11.3944	11.3830	11.3555
		Gas	12.6479	10.5955	12.2752	12.5209	12.5809	12.5976
		Heat	2.9347	4.3893	2.9580	3.1001	3.0721	3.0754
Total Losses (pu)			3.6722	3.1190	3.3843	3.6154	3.6360	3.6284
Cost (mu)			16388.6511	16402.3627	15964.8911	15754.6403	15751.8705	15730.4677
Objective Function (mu)			18960.5487	18588.6434	18273.8646	18188.8198	18199.4468	18169.6515
Computational Time (s)			29.6453	19.6453	18.8789	18.8837	18.6678	18.5632

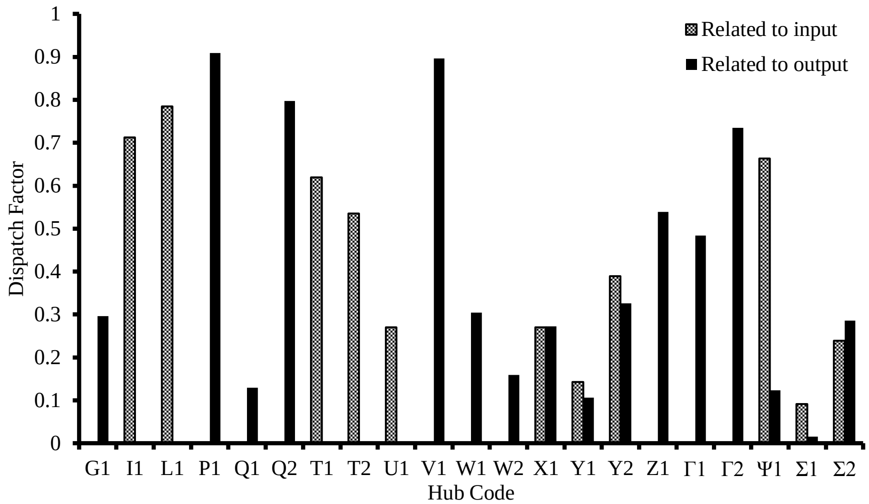

Fig. 13. Dispatch factors of all hubs obtained by SAL-TVAC-GSA for minimization of energy cost and losses

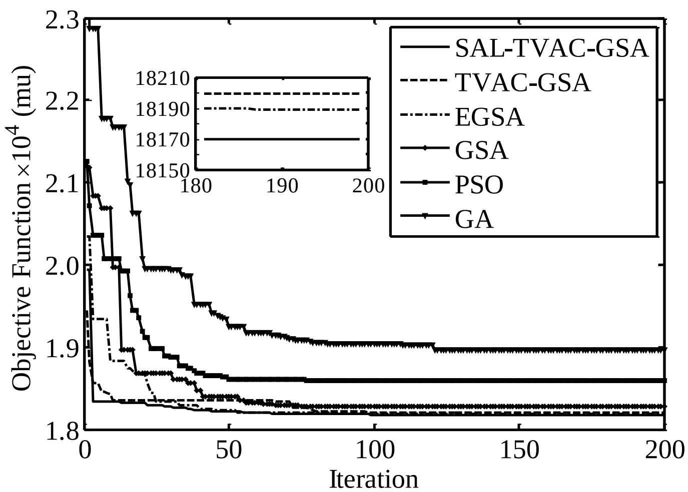

Fig. 14. Convergence characteristics for minimization of energy cost and losses

7. Conclusion

In this paper, SAL-TVAC-GSA as a new and powerful version of GSA was proposed to solve both single- and multi-objective EHED problems. Applying three fundamental modifications to GSA change it to a powerful optimization algorithm which can handle and optimize highly nonlinear, non-convex, non-smooth, non-differential, and high-dimensional EHED problems. Furthermore, a new structure for EHED was proposed and a new complex system including various hubs with different elements and structures was introduced. Moreover, valve-point loading effect for all electrical power-only units and prohibited operating zones for some of them are considered in the problem formulation. For optimization purpose, three cases are optimized as: the first two cases were minimized energy cost and energy hub losses as two different single-objective EHED problems respectively and the final case was simultaneously considered minimization of energy cost and hub losses as a new multi-objective problem. The obtained results using SAL-TVAC-GSA were compared with those found by TVAC-GSA, EGSA, GSA, PSO, and GA techniques. The comparative results demonstrated that the proposed algorithm can search better quality solution with good convergence characteristics and a computational time fully compatible with operational planning time requirements. The other main advantages of the introduced algorithm are its simplicity of implementation, accuracy and fast convergence to the optimal solution while satisfying all constraints. Moreover, the robustness of the proposed algorithm was tested on five benchmark functions. The obtained results were compared with different well-known techniques and the comparison showed that the proposed SAL-TVAC-GSA gives better results. Considering energy networks and the relevant constraints could be investigated in future research works.

Appendix A

System Data

The under studied system includes 76 sources (electrical, gas, and heat units). Moreover, 39 hubs with 29 different configurations (see Fig. 3) construct this system. Characteristics of this system are tabulated as Table A.1–A.4.

Table A.1. Hub data

Hub Code	Hub Type	Efficiency
A1	#1	$\eta_{T} = 0.99$
A2	#1	$\eta_{T} = 1.00$
B1	#2	$\eta_{CHP_e} = 0.30$, $\eta_{CHP_h} = 0.40$
C1	#3	$\eta_{CHCP_e} = 0.25$, $\eta_{CHCP_h} = 0.35$, $\eta_{CHCP_c} = 0.20$
D1	#4	$\eta_{GF} = 0.75$
E1	#5	$\eta_{HE} = 0.95$
F1	#6	$\eta_{T} = 1.00$, $\eta_{CHP_e} = 0.27$, $\eta_{CHP_h} = 0.41$
F2	#6	$\eta_{T} = 0.98$, $\eta_{CHP_e} = 0.31$, $\eta_{CHP_h} = 0.42$
G1	#7	$\eta_{T} = 1.00$, $\eta_{C_a} = 0.70$, $\eta_{C_h} = 0.20$
H1	#8	$\eta_{T} = 0.98$, $\eta_{CHCP_e} = 0.27$, $\eta_{CHCP_h} = 0.37$, $\eta_{CHCP_c} = 0.20$
I1	#9	$\eta_{GF} = 0.80$, $\eta_{CHP_e} = 0.31$, $\eta_{CHP_h} = 0.38$
J1	#10	$\eta_{HE} = 0.98$, $\eta_{CHP_e} = 0.30$, $\eta_{CHP_h} = 0.42$
K1	#11	$\eta_{HE} = 0.95$, $\eta_{CHCP_e} = 0.25$, $\eta_{CHCP_h} = 0.30$, $\eta_{CHCP_c} = 0.30$
L1	#12	$\eta_{GF} = 0.70$, $\eta_{CHCP_e} = 0.29$, $\eta_{CHCP_h} = 0.35$, $\eta_{CHCP_c} = 0.24$
M1	#13	$\eta_{T} = 0.98$, $\eta_{HE} = 0.90$
N1	#14	$\eta_{T} = 0.95$, $\eta_{GF} = 0.73$
O1	#15	$\eta_{HE} = 0.90$, $\eta_{GF} = 0.75$
P1	#16	$\eta_{CHCP_e} = 0.30$, $\eta_{CHCP_h} = 0.31$, $\eta_{CHCP_c} = 0.29$, $\eta_{C_a} = 0.7$, $\eta_{C_h} = 0.20$
Q1	#17	$\eta_{CHP_e} = 0.30$, $\eta_{CHP_h} = 0.40$, $\eta_{C_a} = 0.70$, $\eta_{C_h} = 0.20$
Q2	#17	$\eta_{CHP_e} = 0.35$, $\eta_{CHP_h} = 0.35$, $\eta_{C_a} = 0.65$, $\eta_{C_h} = 0.23$
R1	#18	$\eta_{T} = 1.00$, $\eta_{HE} = 1.00$, $\eta_{CHCP_e} = 0.36$, $\eta_{CHCP_h} = 0.36$, $\eta_{CHCP_c} = 0.34$
S1	#19	$\eta_{T} = 0.97$, $\eta_{HE} = 1.00$, $\eta_{CHP_e} = 0.32$, $\eta_{CHP_h} = 0.44$
S2	#19	$\eta_{T} = 0.99$, $\eta_{HE} = 0.95$, $\eta_{CHP_e} = 0.26$, $\eta_{CHP_h} = 0.40$
S3	#19	$\eta_{T} = 1.00$, $\eta_{HE} = 1.00$, $\eta_{CHP_e} = 0.30$, $\eta_{CHP_h} = 0.40$
T1	#20	$\eta_{T} = 1.00$, $\eta_{GF} = 0.65$, $\eta_{CHP_e} = 0.35$, $\eta_{CHP_h} = 0.45$
T2	#20	$\eta_{T} = 0.97$, $\eta_{GF} = 0.75$, $\eta_{CHP_e} = 0.30$, $\eta_{CHP_h} = 0.42$
U1	#21	$\eta_{T} = 1.00$, $\eta_{GF} = 0.70$, $\eta_{CHCP_e} = 0.30$, $\eta_{CHCP_h} = 0.31$, $\eta_{CHCP_c} = 0.30$
V1	#22	$\eta_{T} = 0.97$, $\eta_{CHCP_e} = 0.35$, $\eta_{CHCP_h} = 0.37$, $\eta_{CHCP_c} = 0.29$, $\eta_{C_a} = 0.65$, $\eta_{C_h} = 0.30$
W1	#23	$\eta_{T} = 0.99$, $\eta_{CHP_e} = 0.30$, $\eta_{CHP_h} = 0.32$, $\eta_{C_a} = 0.59$, $\eta_{C_h} = 0.21$
W2	#23	$\eta_{T} = 1.00$, $\eta_{CHP_e} = 0.33$, $\eta_{CHP_h} = 0.45$, $\eta_{C_a} = 0.50$, $\eta_{C_h} = 0.30$
X1	#24	$\eta_{T} = 0.98$, $\eta_{GF} = 0.76$, $\eta_{CHCP_e} = 0.33$, $\eta_{CHCP_h} = 0.40$, $\eta_{CHCP_c} = 0.31$, $\eta_{C_a} = 0.60$, $\eta_{C_h} = 0.26$
Y1	#25	$\eta_{T} = 1.00$, $\eta_{GF} = 0.74$, $\eta_{CHP_e} = 0.30$, $\eta_{CHP_h} = 0.40$, $\eta_{C_a} = 0.57$, $\eta_{C_h} = 0.27$
Y2	#25	$\eta_{T} = 0.98$, $\eta_{GF} = 0.70$, $\eta_{CHP_e} = 0.35$, $\eta_{CHP_h} = 0.47$, $\eta_{C_a} = 0.62$, $\eta_{C_h} = 0.20$
Z1	#26	$\eta_{T} = 1.00$, $\eta_{HE} = 0.69$, $\eta_{CHCP_e} = 0.30$, $\eta_{CHCP_h} = 0.43$, $\eta_{CHCP_c} = 0.26$, $\eta_{C_a} = 0.63$, $\eta_{C_h} = 0.23$
Γ1	#27	$\eta_{T} = 1.00$, $\eta_{HE} = 0.73$, $\eta_{CHP_e} = 0.32$, $\eta_{CHP_h} = 0.41$, $\eta_{C_a} = 0.60$, $\eta_{C_h} = 0.20$
Γ2	#27	$\eta_{T} = 0.96$, $\eta_{HE} = 0.77$, $\eta_{CHP_e} = 0.26$, $\eta_{CHP_h} = 0.36$, $\eta_{C_a} = 0.55$, $\eta_{C_h} = 0.28$
Ψ1	#28	$\eta_{T} = 0.96$, $\eta_{HE} = 0.90$, $\eta_{GF} = 0.70$, $\eta_{CHCP_e} = 0.26$, $\eta_{CHCP_h} = 0.32$, $\eta_{CHCP_c} = 0.27$, $\eta_{C_a} = 0.55$, $\eta_{C_h} = 0.28$
Σ1	#29	$\eta_{T} = 1.00$, $\eta_{HE} = 0.95$, $\eta_{GF} = 0.78$, $\eta_{CHP_e} = 0.38$, $\eta_{CHP_h} = 0.46$, $\eta_{C_a} = 0.53$, $\eta_{C_h} = 0.32$
Σ2	#29	$\eta_{T} = 1.00$, $\eta_{HE} = 0.95$, $\eta_{GF} = 0.78$, $\eta_{CHP_e} = 0.38$, $\eta_{CHP_h} = 0.46$, $\eta_{C_a} = 0.53$, $\eta_{C_h} = 0.32$

Table A.2. Data of energy sources (units)

Hub Code	Hub Type	Cost Coefficients of Entire Energy					Energy Production Limits (pu)		Entire Energy
		a (mu)	b (mu/pu)	c (mu/pu^2)	d (rad/pu)	e (mu)	$E_{\min}$	$E_{\max}$	
A1	#1	80	200	25	100	4.2	0.10	0.75	Electricity
A2	#1	10	200	120	180	3.7	0.40	2.50	Electricity
B1	#2	20	150	65	-	-	0.50	3.40	Gas
C1	#3	25	100	55	-	-	0.30	3.00	Gas
D1	#4	17	120	60	-	-	0.10	1.10	Gas
E1	#5	10	250	100	-	-	0.20	0.50	Heat
F1	#6	30	180	60	140	4.0	0.20	1.25	Electricity
		20	170	90	-	-	0.10	1.00	Gas
F2	#6	12	210	100	160	3.8	0.30	1.75	Electricity
		25	100	40	-	-	0.10	1.40	Gas
G1	#7	18	190	110	130	4.1	0.10	1.00	Electricity
H1	#8	70	160	100	130	3.3	0.20	1.50	Electricity
		25	100	40	-	-	0.20	1.90	Gas
I1	#9	25	120	50	-	-	0.15	1.00	Gas
J1	#10	20	150	60	-	-	0.10	1.10	Gas
		10	200	110	-	-	0.20	0.50	Heat
K1	#11	20	150	60	-	-	0.10	1.10	Gas
		10	200	110	-	-	0.20	0.50	Heat
L1	#12	25	100	55	-	-	0.30	3.00	Gas
M1	#13	80	200	25	100	4.2	0.10	0.75	Electricity
		15	150	200	-	-	0.10	0.90	Heat
N1	#14	80	200	25	100	4.2	0.10	0.75	Electricity
		25	100	40	-	-	0.20	1.90	Gas
O1	#15	15	150	200	-	-	0.10	0.90	Heat
		20	170	90	-	-	0.10	1.00	Gas
P1	#16	10	220	60	-	-	0.10	3.20	Gas
Q1	#17	19	170	150	-	-	0.10	3.20	Gas
Q2	#17	12	200	70	-	-	0.20	2.70	Gas
R1	#18	12	200	110	120	4.8	0.30	1.75	Electricity
		25	110	70	-	-	0.10	1.40	Gas
		15	150	200	-	-	0.10	0.90	Heat
S1	#19	10	220	160	190	3.6	0.20	1.10	Electricity
		20	200	100	-	-	0.20	1.80	Gas
		12	170	210	-	-	0.10	0.70	Heat
S2	#19	40	190	220	190	4.0	0.10	2.10	Electricity
		34	235	185	-	-	0.10	1.00	Gas
		20	120	410	-	-	0.10	0.90	Heat
S3	#19	80	280	420	220	3.3	0.10	1.80	Electricity
		13	140	185	-	-	0.10	3.00	Gas
		40	220	110	-	-	0.10	1.50	Heat
T1	#20	80	200	25	100	4.2	0.10	0.75	Electricity
		25	100	55	-	-	0.30	3.00	Gas
T2	#20	90	170	230	70	3.9	0.10	1.75	Electricity
		20	90	65	-	-	0.30	3.00	Gas
U1	#21	90	170	230	70	3.9	0.10	1.75	Electricity
		20	90	65	-	-	0.30	3.00	Gas
V1	#22	40	240	180	130	3.6	0.20	1.20	Electricity
		30	70	100	-	-	0.10	2.30	Gas
W1	#23	80	200	25	100	4.2	0.10	0.75	Electricity
		25	100	40	-	-	0.20	1.90	Gas
W2	#23	12	200	110	120	4.8	0.30	1.75	Electricity
		25	110	70	-	-	0.10	1.40	Gas
X1	#24	50	200	110	150	4.4	0.20	1.10	Electricity
		35	190	120	-	-	0.20	1.80	Gas
Y1	#25	28	80	490	100	3.5	0.00	3.00	Electricity
		31	100	220	-	-	0.10	2.80	Gas
Y2	#25	33	175	360	90	4.4	0.00	2.70	Electricity
		39	170	160	-	-	0.10	2.00	Gas
Z1	#26	70	220	310	130	4.6	0.10	2.10	Electricity
		27	230	100	-	-	0.10	1.80	Gas
		10	100	200	-	-	0.10	0.70	Heat

Γ1	#27	95	130	300	90	4.9	0.20	1.90	Electricity
		29	220	330	-	-	0.20	1.00	Gas
		32	135	110	-	-	0.10	0.50	Heat
Γ2	#27	60	230	410	130	3.5	0.10	1.10	Electricity
		50	140	290	-	-	0.20	1.80	Gas
		20	215	220	-	-	0.20	1.70	Heat
Ψ1	#28	20	100	500	310	3.8	0.00	0.90	Electricity
		60	195	85	-	-	0.10	3.80	Gas
		48	265	380	-	-	0.20	1.40	Heat
Σ1	#29	100	150	110	60	4.3	0.10	3.00	Electricity
		20	230	90	-	-	0.10	1.00	Gas
		70	100	40	-	-	0.10	0.40	Heat
Σ2	#29	30	200	160	160	3.2	0.20	1.60	Electricity
		60	110	160	-	-	0.10	4.50	Gas
		30	210	40	-	-	0.10	0.80	Heat

Table A.3. Prohibited zones of electrical power sources (electrical generator units)

Hub Code	Hub Type	Prohibited Zones (pu)
A1	#1	[0.30, 0.35] [0.40, 0.50] [0.65, 0.70]
A2	#1	[0.80, 0.90] [1.50, 1.70] [2.00, 2.10]
G1	#7	[0.50, 0.60] [0.70, 0.80]
M1	#13	[0.30, 0.40] [0.60, 0.65]
V1	#22	[0.30, 0.35] [0.75, 0.80] [1.00, 1.05]
Y1	#25	[1.00, 1.10] [2.00, 2.10]
Σ1	#29	[0.40, 0.50] [1.00, 1.20] [2.50, 2.60]
Σ2	#29	[0.80, 0.90] [1.30, 1.35]

Table A.4. Total demands

Carrier	Demand (pu)
Electricity	12.0
Heat	9.5
Cool	0.7
Compressed Air	1.2

Appendix B

Performance evaluation of SAL-TVAC-GSA on five benchmark functions

Five benchmark functions are selected to evaluate the SAL-TVAC-GSA performance. The results are compared with GA, PSO, TVAC-GSA, and GSA techniques. Data of these functions is adopted from [16].

Results of 50 independent runs are summarized in Table B.1. Accordingly, the obtained SAL-TVAC-GSA results in terms of mean and standard deviations, demonstrate that the proposed optimization algorithm finds the better results (close to the global minimum) on benchmark functions than all other presented algorithms.

Table B.1. Comparison of different algorithm mean and standard deviation for benchmark functions

Functions	GA [45]		PSO [45]		GSA [16]		TVAC-GSA [16]		SAL-TVAC-GSA	
	Mean	Std.	Mean	Std.	Mean	Std.	Mean	Std.	Mean	Std.
f_1	338.5516	361.4970	37.3582	32.1436	5.9908×10^{-4}	1.2315×10^{-4}	2.0145×10^{-6}	9.9037×10^{-7}	1.9627×10^{-6}	1.0049×10^{-8}
f_2	9749.9145	2594.9593	1.1979×10^{-3}	2.1109×10^{-3}	1.9094×10^{-5}	5.2031×10^{-5}	4.1744×10^{-7}	1.6791×10^{-8}	4.1123×10^{-7}	1.5539×10^{-8}
f_3	3.6970	1.9517	0.1460	0.4182	$\ll10^{-300}$	$\ll10^{-300}$	$\ll10^{-300}$	$\ll10^{-300}$	$\ll10^{-300}$	$\ll10^{-300}$
f_4	-1.0298	3.1314×10^{-3}	-1.0160	1.2786×10^{-2}	-1.0316283219	6.7103×10^{-6}	-1.0316283597	6.7752×10^{-9}	-1.03162845348	3.1012×10^{-9}
f_5	7.9610	1.5063	0.4123	0.2500	1.6627×10^{-17}	2.3145×10^{-16}	3.3201×10^{-27}	1.7611×10^{-29}	1.5700×10^{-28}	8.1295×10^{-31}

References

[1] Moeini-Aghtaie M, Abbaspour A, Fotuhi-Firuzabad M, Hajipour E. A decomposed solution to multiple-energy carriers optimal power flow. IEEE Trans Power Syst 2014;29:707–16.

[2] Geidl M, Andersson G. Optimal power flow of multiple energy carriers. IEEE Trans Power Syst 2007;22:145–55.

[3] Shabanpour-Haghighi A, Seifi AR. Effects of district heating networks on optimal energy flow of multi-carrier systems. Renew Sustain Energy Rev 2016;59:379–87.

[4] Shabanpour-Haghighi A, Seifi AR. Energy flow optimization in multicarrier systems. IEEE Trans Ind Informatics 2015;11:1067–77.

[5] Wu J, Yan J, Jia H, Hatziargyrio N, Djilali N, Sun H. Integrated Energy Systems. Appl Energy 2016;166:155–7.

[6] Derafshi Beigvand S, Abdi H, La Scala M. Combined heat and power economic dispatch problem using gravitational search algorithm. Electr Power Syst Res 2016;133:160–72.

[7] Lund R, Vad Mathiesen B. Large combined heat and power plants in sustainable energy systems. Appl Energy 2015;142:389–95.

[8] Fang T, Lahdelma R. Optimization of combined heat and power production with heat storage based on sliding time window method. Appl Energy 2016;162:723–32.

[9] Smith AD, Mago PJ. Effects of load-following operational methods on combined heat and power system efficiency. Appl Energy 2014;115:337–51.

[10] Gu W, Wu Z, Bo R, Liu W, Zhou G, Chen W, et al. Modeling, planning and optimal energy management of combined cooling, heating and power microgrid: A review. Int J Electr Power Energy Syst 2014;54:26–37.

[11] Yang M, Lee SY, Chung JT, Kang YT. High efficiency H2O/LiBr double effect absorption cycles with multi-heat sources for tri-generation application. Appl Energy 2017;187:243–54.

[12] Chua KJ, Yang WM, Er SS, Ho CA. Sustainable energy systems for a remote island community. Appl Energy 2014;113:1752–63.

[13] Liu M, Shi Y, Fang F. Optimal power flow and PGU capacity of CCHP systems using a matrix modeling approach. Appl Energy 2013;102:794–802.

[14] Shabanpour-Haghighi A, Seifi AR. Simultaneous integrated optimal energy flow of electricity, gas, and heat. Energy Convers Manag 2015;101:579–91.

[15] Shabanpour-Haghighi A, Seifi AR. Multi-objective operation management of a multi-carrier energy system. Energy 2015;88:430–42.

[16] Derafshi Beigvand S, Abdi H, La Scala M. Optimal operation of multicarrier energy systems using time varying acceleration coefficient gravi-tational search algorithm. Energy 2016;114:253–65.

[17] Skarvelis-Kazakos S, Papadopoulos P, Unda IG, Gorman T, Belaidi A, Zigan S. Multiple energy carrier optimisation with intelligent agents. Appl Energy 2016;167:323–35.

[18] Pan Z, Guo Q, Sun H. Interactions of district electricity and heating systems considering time-scale characteristics based on quasi-steady multi-energy flow. Appl Energy 2016;167:230–43.

[19] Liu X, Wu J, Jenkins N, Bagdanavicius A. Combined analysis of electricity and heat networks. Appl Energy 2016;162:1238–50.

[20] Li J, Fang J, Zeng Q, Chen Z. Optimal operation of the integrated electrical and heating systems to accommodate the intermittent renewable sources. Appl Energy 2016;167:244–54.

[21] Liu X, Mancarella P. Modelling, assessment and Sankey diagrams of integrated electricity-heat-gas networks in multi-vector district energy systems. Appl Energy 2016;167:336–52.

[22] Xu X, Jin X, Jia H, Yu X, Li K. Hierarchical management for integrated community energy systems. Appl Energy 2015;160:231–43.

[23] Geidl M, Koeppel G, Favre-Perrod P, Klockl B, Andersson G, Frohlich K. Energy hubs for the future. IEEE Power Energy Mag 2007;5:24–30.

[24] Krause T, Andersson G, Frohlich K, Vaccaro A. Multiple-energy carriers: modeling of production, delivery, and consumption. Proc IEEE 2011;99:15–27.

[25] Najafi A, Falaghi H, Contreras J, Ramezani M. Medium-term energy hub management subject to electricity price and wind uncertainty. Appl Energy 2016;168:418–33.

[26] Moeini-Aghtaie M, Dehghanian P, Fotuhi-Firuzabad M, Abbaspour A. Multiagent genetic algorithm: an online probabilistic view on economic dispatch of energy hubs constrained by wind availability. IEEE Trans Sustain Energy 2013;5:699–708.

[27] Li G, Zhang R, Jiang T, Chen H, L. Bai XL. Security-constrained bi-level economic dispatch model for integrated natural gas and electricity systems considering wind power and power-to-gas process. Appl Energy 2016.

[28] Srinivasa Reddy A, Vaisakh K. Shuffled differential evolution for large scale economic dispatch. Electr Power Syst Res 2013;96:237–45.

[29] Subbaraj P, Rengaraj R, Salivahanan S. Enhancement of combined heat and power economic dispatch using self adaptive real-coded genetic algorithm. Appl Energy 2009;86:915–21.

[30] Geidl M. Integrated Modeling and Optimization of Multi-Carrier Energy Systems. ETH Zurich, 2007.

[31] Orehounig K, Evins R, Dorer V. Integration of decentralized energy systems in neighbourhoods using the energy hub approach. Appl Energy 2015;154:277–89.

[32] Geidl M, Andersson G. A modeling and optimization approach for multiple energy carrier power flow. IEEE Russ. Power Tech, St. Petersburg, Russian Federation: 2005, p. 1–7.

[33] Geidl M, Andersson G. Optimal power dispatch and conversion in systems with multiple energy carriers. 15th Power Syst. Comput. Conf., Liège, Belgium: 2005.

[34] Bhattacharya A, Roy PK. Solution of multi-objective optimal power flow using gravitational search algorithm. IET Gener Transm Distrib 2012;6:751–63.

[35] Basu M. Group search optimization for combined heat and power economic dispatch. Int J Electr Power Energy Syst 2016;78:138–47.

[36] Rashedi E, Nezamabadi-pour H, Saryazdi S. GSA: a gravitational search algorithm. Inf Sci (Ny) 2009;179:2232–48.

[37] Marzband M, Ghadimi M, Sumper A, Domínguez-García JL. Experimental validation of a real-time energy management system using multi-period gravitational search algorithm for microgrids in islanded mode. Appl Energy 2014;128:164–74.

[38] Ganesan T, Elamvazuthi I, Shaari KZK, Vasant P. Swarm intelligence and gravitational search algorithm for multi-objective optimization of synthesis gas production. Appl Energy 2013;103:368–74.

[39] Abdi H, Derafshi Beigvand S. Long-term load forecasting based on gravitational search algorithm. J Intell Fuzzy Syst 2016;30:3633–43.

[40] Walsh TB. Effects of rotational motion on the ballistic coefficient of space debris. Auburn University, 2012.

[41] Mohammadi-Ivatloo B, Moradi-Dalvand M, Rabiee A. Combined heat and power economic dispatch problem solution using particle swarm optimization with time varying acceleration coefficients. Electr Power Syst Res 2013;95:9–18.

[42] Ghavidel S, Aghaei J, Muttaqi KM, Heidari A. Renewable energy management in a remote area using modified gravitational search algorithm. Energy 2016;97:391–9.

[43] Narimani MR, Azizi Vahed A, Azizipanah-Abarghooee R, Javidsharifi M. Enhanced gravitational search algorithm for multi-objective distribution feeder reconfiguration considering reliability, loss and operational cost. IET Gener Transm Distrib 2013;8:55–69.

[44] Wang Y, Li B, Weise T, Wang J, Yuan B, Tian Q. Self-adaptive learning based particle swarm optimization. Inf Sci (Ny) 2011;181:4515–38.

[45] He S, Wu QH, Saunders JR. Group search optimizer: an optimization algorithm inspired by animal searching behavior. IEEE Trans Evol Comput 2009;13:973–90.